Taxonomic and paleobiological insights into small mammals from the Pliocene of Western Turkey: a comprehensive study of the locality of Afşar

Skandalos, P.

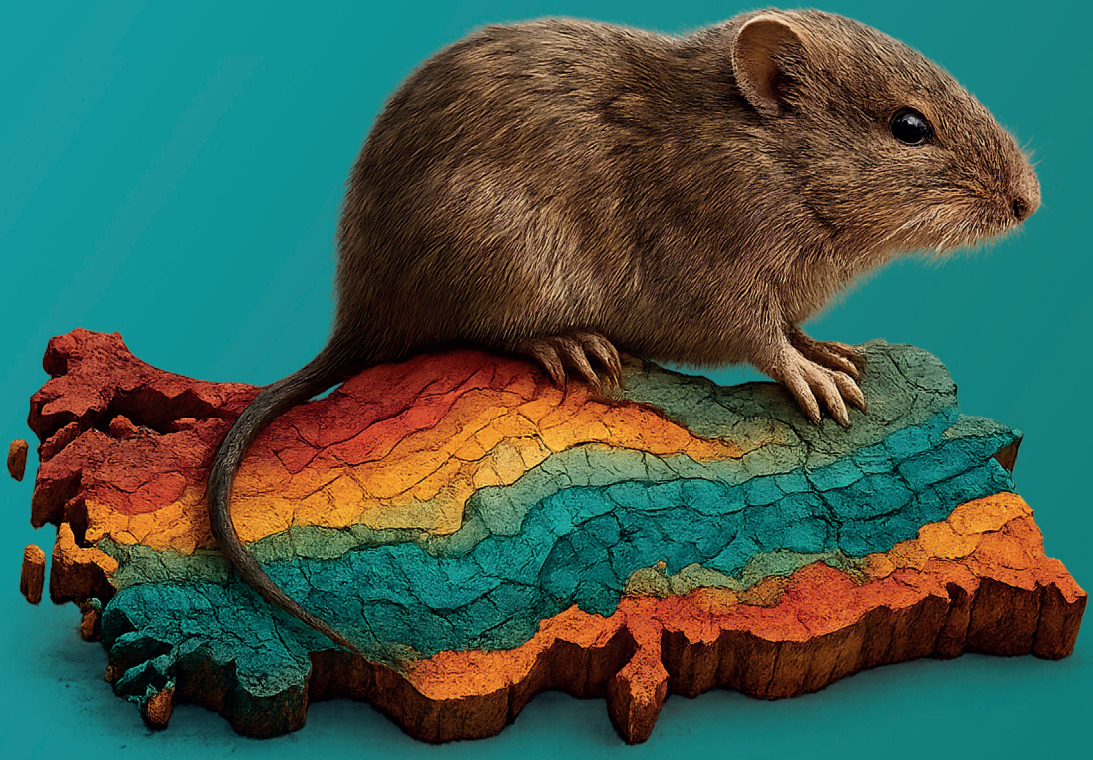

CHAPTER 2

Early Pliocene Arvicolinae and Cricetinae from the locality of Afşar, Western Turkey

Panagiotis Skandalos[1,2,*], Koen Iansing[2], Fatma Arzu Demirel[3], Mehmet Cihat Alçiçek[4], Serdar Aayda[5], Francien Eveleijntje Dieleman[1,] Lars W. van den Hoek Ostende[1]

[1]Naturalis Biodiversity Center, Leiden, the Netherlands

[2]Institute of Biology, Leiden University, Leiden, the Netherlands

[3]Department of Anthropology, Burdur Mehmet Akif Ersoy University, Burdur, Turkey

[4]Department of Geology, Pamukkale University, Denizli, Turkey

[5]Department of Biology, Ege University, İzmir, Turkey

Received: 29.07.2022 | Accepted/Published Online: 23.10.2022 | Final Version: 19.01.2023

Abstract

The Afşar section, situated in the Dombayova graben in Western Turkey, is one of the key localities for the study of the Pliocene of Anatolia. Two fossiliferous layers yielded micromammal assemblages, including various cricetine and arvicoline species. These include the species *Mimomys* cf. *gracilis*, *Pliomys* sp., Arvicolinae gen. sp. and the cricetines *Cricetulus* cf. *ehiki* and *Cricetulus* sp. in Afşar 1 and *Mimomys hassiacus*, *M. gracilis*, *Pliomys graecus* and *Mesocricetus primitivus* in Afşar 2. The cooccurence of these species indicates a dry and open spaced habitat. Based on the composition and stage of evolution of the hamster and vole species, Afşar 1 assemblage can be referred to MN 15 or early MN 16 with Afşar 2 being assigned to early MN 16.

Key words: Biostratigraphy, Anatolia, *Mesocricetus, Cricetulus, Mimomys, Pliomys*

1. Introduction

The Late Pliocene–Early Pleistocene is a transitional period for the paleoenvironment of Southwestern Anatolia. During that period, Southwestern Turkey had an open and steppe environment with vegetation limited to the surroundings of paleolakes and close to the shores of the Mediterranean Sea (Jiménez-Moreno et al., 2005; Suc and Popescu, 2005; Jiménez-Moreno et al., 2010, 2015). The warm and seasonally arid environment, which started from the Middle Miocene onwards, was succeeded by cooler conditions and a humid–arid alternation during the Pliocene (Eronen et al., 2009; Jiménez-Moreno et al., 2015), eventually leading to the glacial–interglacial cycles of the Pleistocene (Popescu et al., 2010). The transition period from the Miocene to the Pliocene is characterised by an important role in the enrichment of the Eurasian vertebrate faunas (Koufos, 2013; Koufos and Vasileiadou, 2015; Koufos, 2016; Hoek Ostende et al., 2020). However, our knowledge about the Miocene of Anatolia (e.g., De Bruijn et al., 2006; Kaya et al., 2007; Bilgin et al., 2021, 2022) is much larger compared to that about the Pliocene. Despite a large number of Turkish Pliocene localities existing (Ünay and De Bruijn, 1998), the fossil record is still mainly unpublished (Hoek Ostende et al., 2015). This holds particularly true for the micromammals.

During recent field campaigns of the project "Surveys for the identification of fossil localities of Neogene and Pleistocene periods in the province of Afyon and Burdur" led by one of us (FAD), a large number of promising new localities were found. The study of the micromammals of these localities is part of the PhD thesis of the first author (PS). Among the new localities, the Afşar section is of special importance. It was recognized as a fossil mammal locality in the early 1990s by an MTA (Mineral Research and Exploration General Directorate) geologist Gerçek Saraç and features in his technical report on Anatolian mammal localities as Afyon–Sandıklı–Afşar (Saraç, 2003). The site was revisited in the framework of the Afyon and Burdur survey in 2017 (Demirel et al., 2019) and subsequently sampled by one of us (MCA) from Pamukkale University, at which time two different fossiliferous layers were recognized. These are indicated as Afşar 1, situated at the lower part of the section, and Afşar 2, at the upper part of the section. The presence of two assemblages in superposition well separated in time is important, as it allows us to document successive changes in the composition and evolutionary levels of the assemblages. Based on the current research, the Afşar assemblages comprise murines, arvicolines, cricetines, gerbils, glirids, spalacines, lagomorphs, and insectivores, as well as large mammals with equids (Hipparion), cervids, and carnivores (Baranogale).

In this paper, we describe the Cricetinae and Arvicolinae from the Afşar assemblages. Particularly the latter are excellent stratigraphic markers for dating the Plio-Pleistocene assemblages and are therefore an important tool to date also the Afşar assemblages. However, despite their dominance in numerous Pliocene localities, detailed descriptions of both groups are usually rare. One of the clear evolutionary trends in Arvicolinae is their successive increase of crown height (hypsodonty). Rabeder (1981, 1988) demonstrated that the hypsodonty of the molars can be quantified by describing and measuring the enamel-free area (=linea sinuosa). Since then, many researchers have proved the importance of

this character (e.g., Maul et al., 1998; Tesakov, 2004, Zhang et al., 2010). However, particularly in older literature, a detailed description of the arvicoline's enamel-free areas is rare, more often than not limited to Hsd/L. This may provide an extra challenge particularly when identifying Pliocene representatives of the subfamily. In our description of the Afşar voles, we will provide a particular reference to the linea sinuosa.

1.1 Geology

Western Anatolia is a territory of postorogenic crustal extensions from the Late Tortonian onward and prominent with a broad array of NE-trending basins represented by a synchronic, rather uniform superimposition of alluvial, fluvial, and lacustrine sediments (Alçiçek et al., 2019). Among these basins, the N-NW trending Dombayova graben hosting the Afşar locality resides on a Mesozoic– Paleogene basement and is composed of Upper Miocene to Quaternary terrestrial sediments (Cihan et al., 2003; Balcı, 2011) (Figure 1). The tripartite sedimentation sequence in the Dombayova graben comprises alluvial-fan, fluvial, and lacustrine deposits that overlie each other in a layer-cake style in the basin centre, interfingering laterally towards the basin margins. Sedimentation in the basin is documented by a transition from alluvial fans and axial fluvial systems into central lakes. The lignitic marsh-swamp deposits of Afşar, combined with the high number of desman fossils present in the assemblages, suggest humid local conditions during the Pliocene. Later on, the basin further subsided by subsequently deepening of the lakes as documented by thick and laterally extensive marly carbonate successions. The lakes later shrank due to renewed progradation of alluvial-fans and eventually filled up and dried out, reflected by marsh-swamp deposits at the top of a complete lacustrine succession that contain a diverse micromammal assemblage referable to MN16 in the locality of Gülyazı (Sickenberg et al., 1975). The Afşar locality is situated near Afşar village in Afyonkarahisar Province of Turkey, where some coal exploration was active during the last century. The assemblage mentioned in the technical report of Saraç (2003) is located in the coal mine lying at the bottom of the lacustrine succession. Afşar 1 was sampled from the same part of the section, while Afşar 2 is located several metres higher, at the top of the same lacustrine succession.

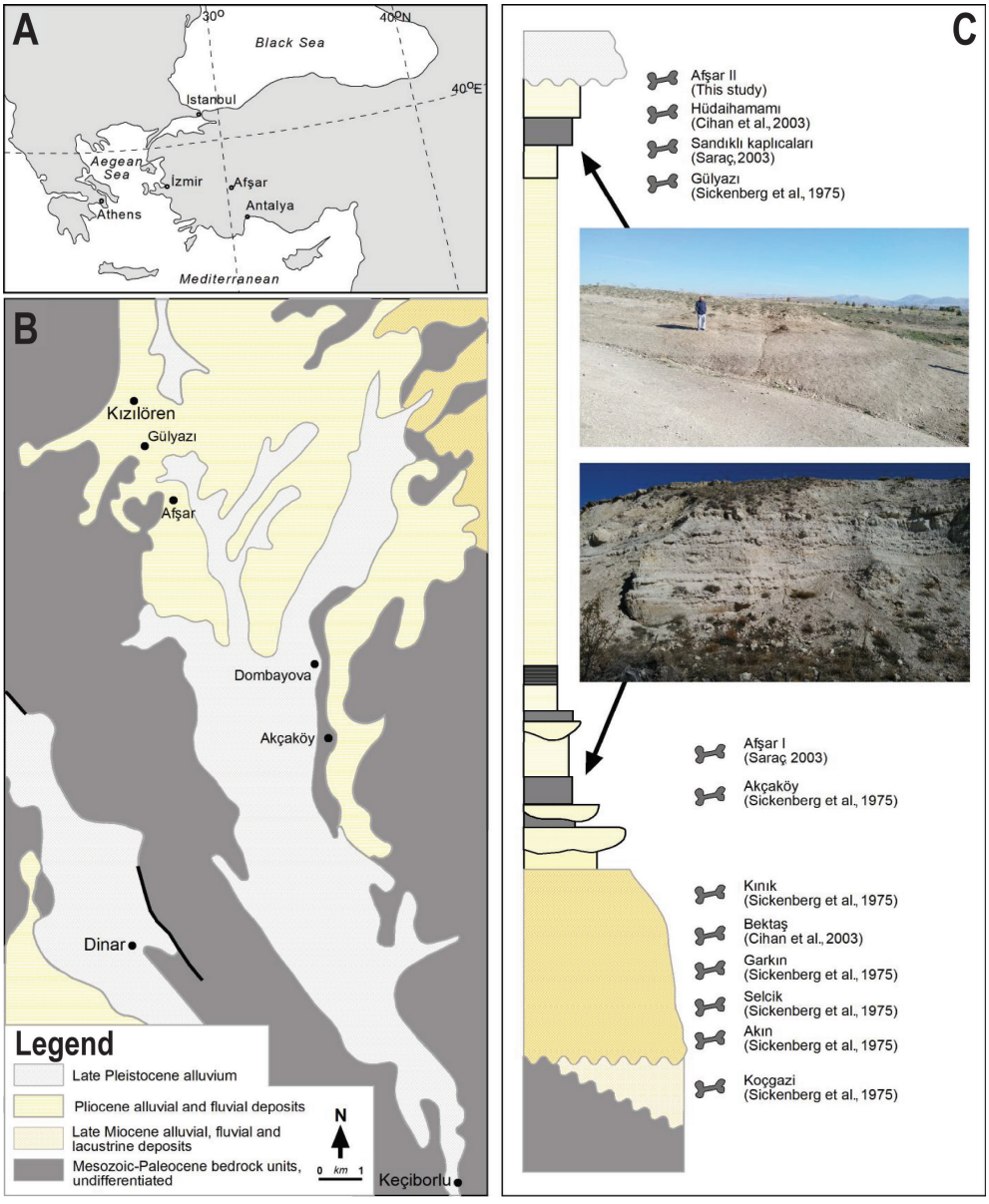

Figure 1. (A) Geographic position of the Afşar locality. (B) Geological map of the Dombayova Graben with the Afşar locality (after Turan, 2002). (C) Stratigraphy of Dombayova Graben based on the fossil data by Saraç (2003), Cihan et al. (2003), Balcı (2011) and this study.

2. Material and methods

All material was collected by wet screening on a set of sieves with the finest mesh of 0.5 mm. It includes 26 Cricetinae molars from which 8 (1 M1; 2 M2; 1 m1; 2 m2; 2 m3) come from the lower layer (Afşar 1) and 18 (1 M1; 4 M2; 2 M3; 6 m1; 2 m2; 3 m3) from the upper one (Afşar 2). Arvicolinae are represented by 345 molars from which 33 (7 M1; 3 M2; 2 M3, 3 m1; 12 m2; 6 m3) come from Afşar 1 and 312 (54 M1; 46 M2; 43 M3; 65 m1; 55 m2; 49 m3) from Afşar 2 (Table 1). The complete collection of this locality is stored in the Natural Museum of Ege University of İzmir in Turkey.

The nomenclature used for Cricetinae molars (Figures 2 and 3) follows López-Guerrero et al. (2013), that used for the Arvicolinae (Figures 4–13) follows Van der Meulen (1973) and Rabeder (1981). Photographs were taken with a Leica 16A microscope with Leica application suite software. The following measures were taken from the photographs: AL: Length of the Anteroconid complex, AS: height of the anterosinus, ASD: height of the anterosinuid, HSD: height of the hyposinuid, HSLD: height of the hyposinulid, L: maximum length of the occlusal surface, PRS: height of the protosinus, W: width of the occlusal surface. We calculated the PA-index $=\sqrt{PRS^2+AS^2}$ (protosinus-anterosinus height) and HH-index= $\sqrt{HSD^2+HSLD^2}$ (hyposinuid-hyposinulid height) according to Rabeder (1981). Comparative material comprises 35 m1 of *Mimomys occitanus* Thaler, 1955 from its type locality of Séte, in France (SE 251 to 285) and 14 m1 (TB1 681 to 691; TB1 693; TB1 694; TB1 699) and 20 M3 (TB1 761 to 770; TB1 A761 to A770) of *Pliomys graecus* De Bruijn and Van der Meulen, 1975 from the locality of Toukobounia-1, stored in the Department of Earth Sciences in Utrecht University in the Netherlands.

Table 1. List of the Cricetinae and Arvicolinae species identified in Afşar.

Locality	Subfamily	Species	N
Afşar 2	Cricetinae	*Mesocricetus primitivus*	18
	Arvicolinae	*Mimomys hassiacus*	57
		Mimomys gracilis	51
		Pliomys graecus	204
	Cricetinae	*Cricetulus* cf. *ehiki*	5
		Cricetulus sp.	3
Afşar 1	Arvicolinae	*Mimomys* cf. gracilis	6
		Pliomys sp.	26
		Arvicolinae gen. sp.	1

3. Systematic paleontology

Order **Rodentia** Bowdich, 1821
Family **Muridae** Illiger, 1811
Subfamily Cricetinae Fischer, 1817
Genus *Mesocricetus* Nehring, 1898
Mesocricetus primitivus De Bruijn et al., 1970
Type locality: Maritsa I, island of Rhodes, Greece
Locality: Afşar 2
Measurements: Table 2

Table 2. Material and measurements of *Mesocricetus primitivus* from Afşar 2 (mm).

	Length				**Width**			
	N	Min	Max	Mean	N	Min	Max	Mean
M1	1	2.23	2.23	2.23	1	1.42	1.42	1.42
M2	3	1.71	1.84	1.78	3	1.37	1.42	1.40
M3	2	1.40	1.54	1.47	2	1.07	1.19	1.13
m1	3	1.97	2.03	2.00	3	1.18	1.25	1.22
m2	2	1.83	1.93	1.88	2	1.44	1.47	1.45
m3	2	1.73	1.87	1.80	2	1.26	1.40	1.33

Description. M1 (Figure 2H) has a rectangular outline with opposite cusps. The lingual cusps are somewhat wider than the labial ones. The anterocone is clearly divided into two cusps. The two parts are connected to the lingual and the labial part of the anteroloph, respectively. The protolophule I is lower than the protolophule II; both connect to the paracone. The mesoloph is absent. The posteroloph is transverse, ending on the posterolabial border of the molar, behind the metacone. The posterior flank of the latter is damaged, so it is not possible to observe a possible connection with the posteroloph. The roots are not preserved.

M2s (Figures 2I–2J) are subrectangular. The main cusps are positioned opposite, with the lingual ones being wider than the labial ones. The anterolabial cingulum is well developed and encircles a deep anterosinus. The anterolingual cingulum is present as well; in two out of the four specimens, it is more distinct, encircling a thin protosinus. The protolophule I connects with both the anterocone and the paracone. The protolophule II is strongly connected to the paracone. The mesoloph is absent. One of the specimens has an entostyle (PV-AFS-14), on the posterior side of the protocone. The posteroloph encircles a wide posterosinus, ending on the posterior flank of the metacone. The molar has four roots.

M3 (Figure 2K) has a subtriangular outline. Its anterolabial cingulum is well developed, encircling a wide anterosinus. The anterolingual cingulum is absent. The protocone is the widest cusp with a small entostyle on its posterior flank in one out of the two specimens. The other molar (PV-AFS-18) is damaged, which makes the observation of the last character impossible. The metacone and the hypocone are both reduced in size, almost being incorporated into their respective lophs. M3 has three roots.

m1s (Figure 2A–2C) are very elongated with slightly alternating main cusps. The anteroconid is divided into a lingual and labial part. One out of the six specimens (PV- AFS-2) has its lingual part wider than the labial one. Two of the specimens (PV-AFS-1, PV-AFS-4) have a wider labial part and two more have parts with almost equal size (PV- AFS-3, PV-AFS-5). The last specimen (PV-AFS-6) is very worn and it is not possible to observe the morphology of the anteroconid. The anterolophulid is single and on its anterior side, it connects to both the parts of the anteroconid. In one specimen (PV-AFS-5), it is connected to the lingual cusp only. The mesolophid is absent and the wide mesosinusid is L-shaped. In three out of the four specimens (PV-AFS-1, PV-AFS-3, PV-AFS-6), an inconspicuous ectostylid is present, the other two are damaged in that area. The posterolophid is developed backwards, bounding a wide and open posterosinusid. The molar has a wide and transverse posterior root and smaller anterior one.

m2s (Figures 2D and 2E) have a rectangular outline. The main cusps are slightly alternating. The anterolabial cingulum is well developed bordering a wide protosinusid. The anterolingual cingulum is absent. The protoconid and the hypoconid are slightly wider than their opposite cuspids. Both specimens have a medium-sized mesolophid, which ends freely in the mesosinusid behind the metaconid. The sinusid is deep and wide with a strong labial cingulum. The posterolophid is curved. It encircles a wide posterosinusid, ending against the entoconid. The molar has two roots.

m3s (Figures 2F and 2G) are subtriangular with slightly alternating cusps. The anterolingual cingulum is almost integrated into the metalophulid and the metaconid. The anterolabial cingulum is well developed and together with the widest cuspid, the protoconid, it borders a wide and deep protosinusid. The mesolophid is medium to long. The entoconid is reduced but keeps its cuspid form. The hypoconid is fused into the posterolophid. In one of the specimens (PV-AFS-9), the posterolophid is curved, ending freely in the posterosinusid. The molar has two roots.

Remarks. The molars of the middle-sized cricetine from Afşar 2 fits well with *Mesocricetus primitivus* from the Greek locality of Maritsa I and the Turkish localities of Bıçakçı and Çalta (De Bruijn et al., 1970; Şen, 1977; Hoek Ostende et al., 2015) (Figures 14–16). However, its m2 is slightly larger and somewhat closer to *M. primitivus* from Silata (Vasileiadou et al., 2003) and *M. auratus* from the Anatolian locality of Meydan (Hír, 1992). In addition, one of the two M3 (PV-AFS-17) seems to be reduced in size. The material from Afşar 2 differs from *M.* aff. *arameus* from Kızıleğrek (Erturaç et al., 2019) by its wider m2 and the smaller m3. Furthermore, it differs from *M. brandti* from Yolpınar (Erturaç et al., 2019) by a smaller m3. Apart from the metrical similarity, the clearly divided anterocone and the connection of the protolophule I to the

metacone of the M1, the well-developed anterosinus of the M2 and M3, the absence of the mesoloph in the upper molars, the wide protosinusid of the m2 and m3 with their well- developed mesolophids, confirm the classification of the hamster from Afşar 2 as *M. primitivus*.

The oversplit of some genera and the excessive use of *Allocricetus* Schaub, 1930, places the taxonomy in flux (Kowalski, 2001; Hordijk and De Bruijn, 2009; López Jiménez et al., 2018). The genus is based on skull characters, with its dentition being similar to *Cricetulus* Milne-Edwards, 1867 (Mayhew, 1978). Hír (1993b) indicates that the morphological difference between the molars of the two genera is observed only by a sufficient sample size. Furthermore, the cladogram made by Cuenca-Bescós (2003, figure 2) shows the morphological similarity between the two genera. Based on the work of these authors, Hoek Ostende (2015) indicates that the differences between *Allocricetus* and *Cricetulus* are sufficient to separate species and not genera. According to the same author, the two hamsters are congeneric. The larger representatives of hamsters seem all to belong to genus *Cricetus* (Leske, 1779), the medium sized ones from SW Europe to *Mesocricetus* Nehring, 1898, and the small ones to *Allocricetulus* Argyropulo, 1932, and *Cricetulus* (Kowalski, 2001). The whole group of Cricetinae is generally connected to an open steppe environment (Musser and Carleton, 1993).

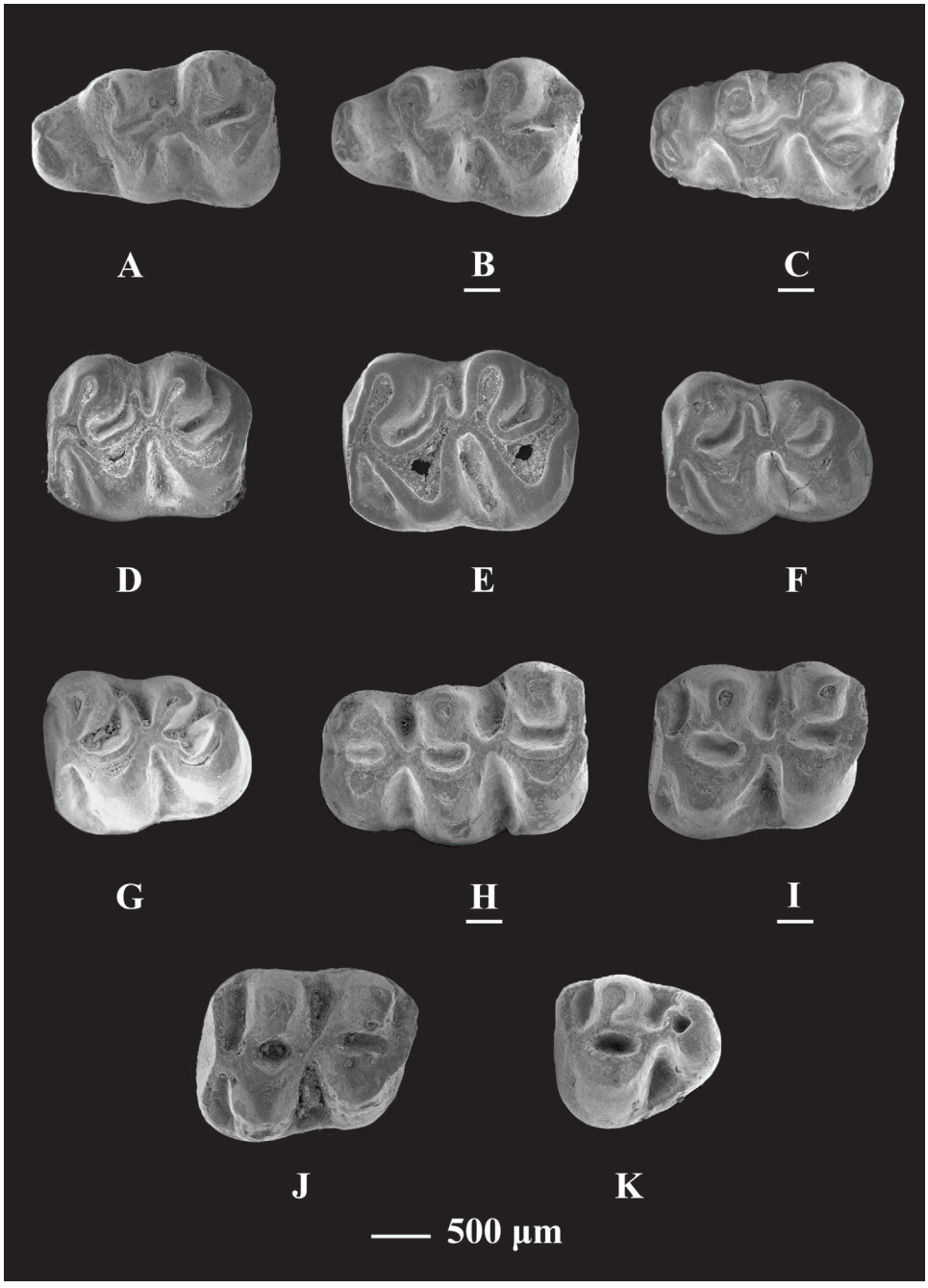

Figure 2. *Mesocricetus primitivus* from Afşar 2. m1: A (PV-AFS-1), B (PV-AFS-3), C (PV-AFS-4): m2: D (PV-AFS-7), E (PV-AFS-8): m3: F (PV-AFS-11), G (PV-AFS-9): M1: H (PV-AFS-12): M2: I (PV-AFS-13), J (PV-AFS-15): M3: K (PV-AFS-17). Underlined letter indicates inversed figure of the specimen.

Genus *Cricetulus* Milne-Edwards, 1867

Cricetulus cf. *ehiki* (Schaub, 1930)

Type locality: Villány (? 5), Kalkberg

Locality: Afşar 1

Measurements: Table 3

Table 3. Material and measurements of *Cricetulus* cf. *ehiki* from Afşar 1 (mm).

	Length				**Width**			
	N	Min	Max	Mean	N	Min	Max	Mean
M1	-	-	-	-	1	1.36	1.36	1.36
M2	-	-	-	-	-	-	-	-
M3	-	-	-	-	-	-	-	-
m1	1	1.95	1.95	1.95	1	1.13	1.13	1.13
m2	1	1.62	1.62	1.62	1	1.31	1.31	1.31
m3	2	1.64	1.72	1.68	2	1.20	1.23	1.21

Description. M1 (Figure 3E) is rectangular. The labial main cusps are slightly wider than their opposite lingual counterparts. The anterior part of the molar is damaged. The anterocone is divided into two cusps. The two parts are connected to the lingual and the labial anteroloph, respectively. The parastyle is present. The protosinus is L-shaped. The protolophule I ends next to the paracone, without a connection. The protolophule II, on the other hand, is strongly connected to the paracone. The mesoloph is absent. A small entostyle is present on the anterolingual face of the hypocone. The posteroloph is transverse, ending on the posterolabial border of the molar. Close to its end, it becomes thicker and connects to the posterior side of the metacone. The roots are not preserved.

m1 (Figure 3A) is elongated, being wider on its posterior side. Despite the sole specimen being very worn, it is possible that the main cusps are slightly alternating. The mesoloph is absent. The posterolophid is developed backwards, ending on the posterolingual side of the molar. The molar has a wide and transverse posterior root and smaller anterior one.

The only available m2 (Figure 3B) is worn and has a rectangular outline with slightly alternating main cuspids. The labial cuspids are wider than the lingual ones. The anterolingual cingulum is absent. The anterolabial cingulum is well developed and curved, encircling a wide, shallow and posteriorly directed protosinusid. The mesolophid is short, ending on the posterior side of the metaconid. The sinusid is very wide with a wide ectostylide on the anterior flank of the hypoconid. The posterolophid is curved; it borders a thin and lingualy open posterosinusid and ends on the posterolingual side of the molar. The molar has two wide and transverse roots.

m3s (Figures 3C and 3D) have a subtriangular outline. Its anterior side is clearly wider than the posterior; its main cuspids are slightly alternating. The anterolabial cingulum is well developed and together with the protoconid, they border a wide and deep protosinusid. The anterolingual cingulum is absent. One of the two specimens (PV-AFS-363) has a long mesolophid, which ends on the posterolingual flank of the metaconid. The other specimen (PV-AFS-364) has a short mesolophid, which also ends behind the metaconid. The entoconid is reduced but keeps its cuspid form. The hypoconid is almost incorporated into the posterolophid. The latter is curved and thin; it encircles a wide posterosinusid and ends on the posterior flank of the entoconid. The molar has two wide roots.

Remarks. The second hamster from Afşar 1 is smaller than *Mesocricetus primitivus* from Afşar 2, and its molars fit well within the size range of *Cricetulus ehiki* from Maramena in Greece (Daxner-Höck, 1992), Tepe Alagöz in Turkey (Čermák et al., 2019), and Villány 3 and Osztramos 3 in Hungary (Figures 17–19) (Hír, 1993a). *Cricetulus ehiki* from Muselievo in Bulgaria (Popov, 2004) is bigger than the molars from Afşar. Only one upper molar, a damaged M1, is preserved. The m1 and m2 are both worn. This damaged and scanty material prevents further implication. Morphologically, the finds are similar to *C. ehiki* (Schaub, 1930). The anterocone of the M1 is divided, the parastyle present and the mesoloph absent, the protosinusid and the ectostylide of the m2 are wide and its mesolophid, although present, is underdeveloped. Based on this morphology, and particularly on the presence of the parastyle (Hír, 1989, 1993b; Cuenca-Bescós, 2003), as well as the size similarity with other *C. ehiki* assemblages, the hamster from Afşar 1 is classified as *C.* cf. *ehiki*. Kowalski (2001) synonymised the genera *Allocricetus* Schaub, 1930, *Cricetinus* Zdansky, 1928, *Cricetiscus* Thomas, 1917, *Phodopus* Miller, 1910, *Rhinocricetus* Kretzoi, 1956, and *Tscherskia* Ognev, 1914, with the extant *Cricetulus* Milne-Edwards, 1867.

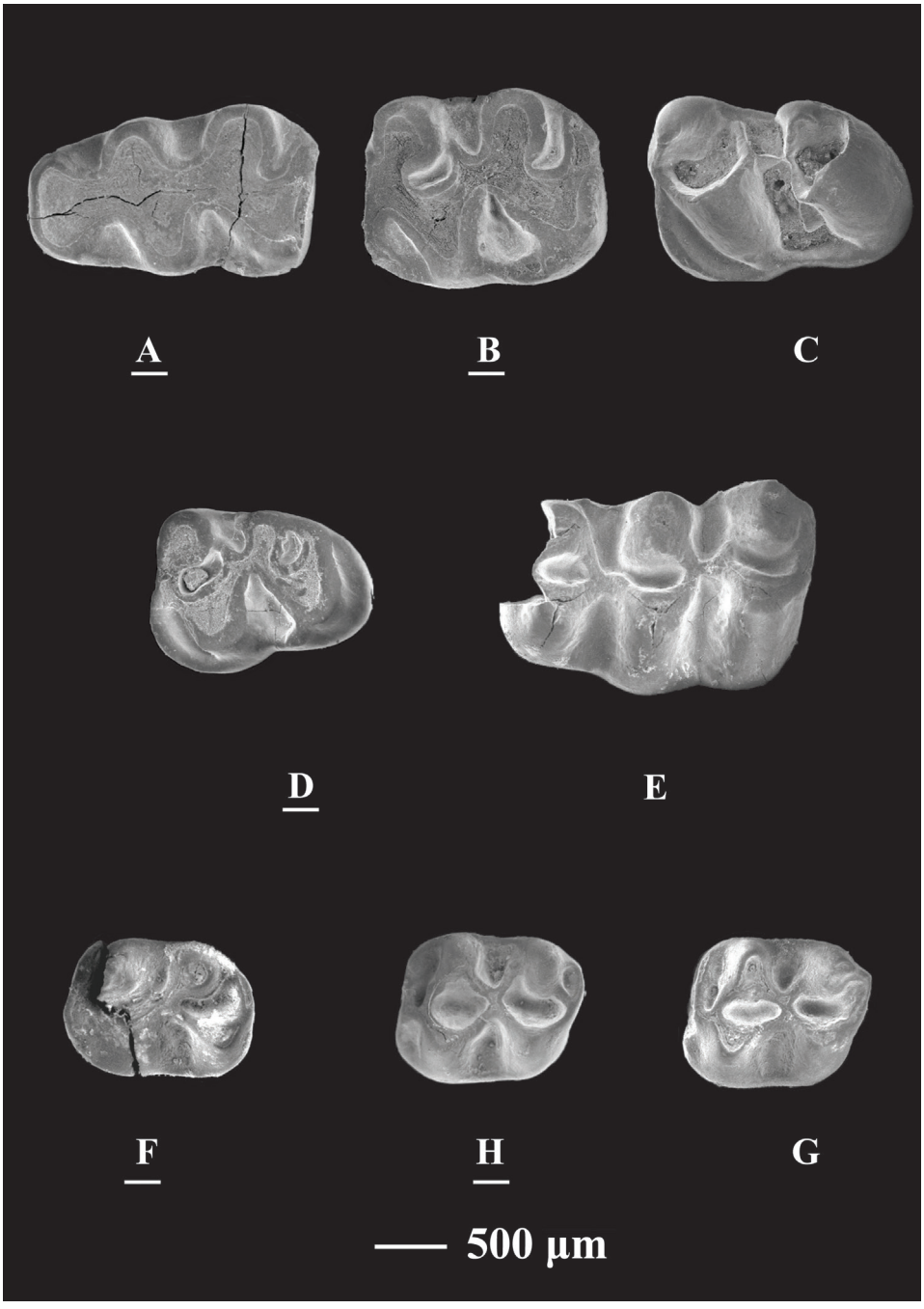

Figure 3. *Cricetulus* cf. *ehiki* from Afşar 1. m1: A (PV-AFS-361), m2: B (PV-AFS-362), m3: C (PV-AFS-363), D (PV-AFS-364), M1: E (PV-AFS-360). *Cricetulus* sp. from Afşar 1. m2: F (PV-AFS-368): M2: H (PV-AFS-367), G (PV-AFS-366). Underlined letter indicates inversed figure of the specimen.

Cricetulus sp.

Locality: Afşar 1

Measurements: Table 4

Table 4. Material and measurements of *Cricetulus* sp. from Afşar 1 (mm).

	Length				**Width**			
	N	Min	Max	Mean	N	Min	Max	Mean
M1	-	-	-	-	-	-	-	-
M2	2	1.24	1.29	1.26	2	0.99	1.01	1.00
M3	-	-	-	-	-	-	-	-
m1	-	-	-	-	-	-	-	-
m2	1	1.26	1.26	1.26	1	0.98	0.98	0.98
m3	-	-	-	-	-	-	-	-

Description. M2s (Figures 3G and 3H) have a trapezoidal outline. The main cusps are almost opposite to each other and are of similar size. The anterolabial cingulum is well developed, encircling a wide anterosinus. In one of the two specimens (PV-AFS-366), the anterolingual cingulum is absent. The second one (PV-AFS-367) has it as a short ridge, bordering a thin protosinus. The paracone is connected with both the protolophule I and protolophule II. The sinus is very wide and the pits between the main cusps are rather deep. The posteroloph is curved and encircles a wide posterosinus, ending on the posterolabial border of the molar. In one of the two specimens (PV-AFS-367), the posterior metaloph ends in the middle of the posteroloph and, in the other one (PV-AFS-366), at the end of that ridge. The molar has four strong roots.

m2 (Figure 3F) is subrectangular with slightly alternating main cuspids. The anterolabial cingulum is well developed and borders a shallow and wide protosinusid. The anterolingual cingulum is present and there are inconspicuous patches of the cingulum at the base of the metaconid. The mesolophid is absent. The mesosinusid is wide and L-shaped and the sinusid very deep. The posterolophid is long, curved, and thin. It encircles the posterosinusid and ends on posterolingual border of the molar. The molar has two wide, long, and vertically developed roots.

Remarks. The two M2 are metrically intermediate between *Calomyscus minor* from Maritsa I in Greece (De Bruijn et al., 1970), *Cricetulus bursae* from Cueva Negra in Spain (López Jiménez et al., 2018) and *Cricetulus migratorius* and *C. bursae* from the Turkish localities of Iğdeli and Bıçakçı (Suata-Alpaslan et al., 2010: Hoek Ostende et al., 2015). The sole m2 fits well in the range of *Calomyscus minor*, which is smaller than the *Cricetulus* species. M2 has the main cusps nearly opposite, and low ridges that encircle their deep pits between them, which is characteristic for *Cricetulus migratorius* from Bıçakçı. Based on the morphological similarity with the *Cricetulus* species and due to the scanty material of the layer, we refer the small hamster only generically to *Cricetulus* sp.

Subfamily **Arvicolinae** Gray, 1821

Genus *Mimomys* Forsyth Major, 1902

Mimomys hassiacus Heller, 1936

Type locality: Gundersheim-1 (Germany)

Locality: Afşar 2

Measurements: Table 5

Table 5. Material and measurements of *Mimomys hassiacus*, Afşar 2 (mm).

M1	**N**	**Min**	**Max**	**Mean**	**Std.Dev.**	**Std.error**
Length	6	2.48	2.84	2.63	0.12	0.05
Width	6	1.54	1.73	1.66	0.08	0.03
AS	4	0.65	0.75	0.70	0.04	0.02
PRS	5	0.92	1.16	1.03	0.09	0.04
PA- index	4	1.14	1.37	1.24	0.09	0.05
M2	**N**	**Min**	**Max**	**Mean**	**Std.Dev.**	**Std.error**
Length	8	1.80	2.20	2.04	0.14	0.05
Width	8	1.24	1.57	1.41	0.10	0.04
AS	5	0.40	0.69	0.54	0.13	0.06
PRS	5	0.33	0.67	0.53	0.14	0.06
PA- index	5	0.61	0.96	0.77	0.15	0.07
M3	**N**	**Min**	**Max**	**Mean**	**Std.Dev.**	**Std.error**
Length	8	1.85	2.05	1.91	0.07	0.02
Width	9	1.04	1.21	1.15	0.06	0.02
AS	7	0.48	0.57	0.53	0.03	0.01
PRS	7	0.22	0.44	0.34	0.08	0.03
L PC	8	0.89	1.09	1.02	0.07	0.02
W PC	9	0.93	1.07	1.01	0.04	0.01
PA- index	6	0.53	0.71	0.63	0.07	0.03
LP/L	8	47.21	57.73	53.28	3.34	1.18
m1	**N**	**Min**	**Max**	**Mean**	**Std.Dev.**	**Std.error**
Length	10	2.75	3.12	2.92	0.12	0.04
Width	9	1.34	1.61	1.46	0.08	0.03
ASD	1	2.21	2.21	2.21	-	-
HSD	7	0.63	1.09	0.90	0.16	0.06
HSLD	10	0.25	0.77	0.48	0.20	0.06
AL	9	32.95	43.05	39.17	3.09	1.03
HH- index	7	0.73	1.29	1.07	0.21	0.08

Table 5. Continued

m2	N	Min	Max	Mean	Std.Dev.	Std.error
Length	7	1.70	2.00	1.88	0.12	0.05
Width	7	1.14	1.48	1.35	0.10	0.04
HSD	6	0.62	0.97	0.80	0.13	0.05
HSLD	5	0.47	0.63	0.55	0.06	0.03
HH- index	5	0.78	1.16	0.99	0.14	0.06
m3	**N**	**Min**	**Max**	**Mean**	**Std.Dev.**	**Std.error**
Length	8	1.67	1.78	1.73	0.04	0.02
Width	8	0.95	1.11	1.06	0.05	0.02
HSD	5	0.33	0.45	0.39	0.05	0.02
HSLD	5	0.33	0.42	0.38	0.03	0.01
HH- index	4	0.49	0.61	0.55	0.06	0.03

Description. M1s (Figures 4a and 4b) have three well- developed roots. One out of the seven specimens (PV-AFS-67) has an additional anterolingual root. The occlusal surface includes the anterior lobe, three wide triangles, and the metacone. The latter comprises the fourth triangle. None of them is isolated with the connection of T1 with T2 being the widest. The enamel differentiation follows the *Mimomys* type and the cement is present in the synclines. The protosinus is the highest enamel-free area, with a maximum height of 1.16 mm.

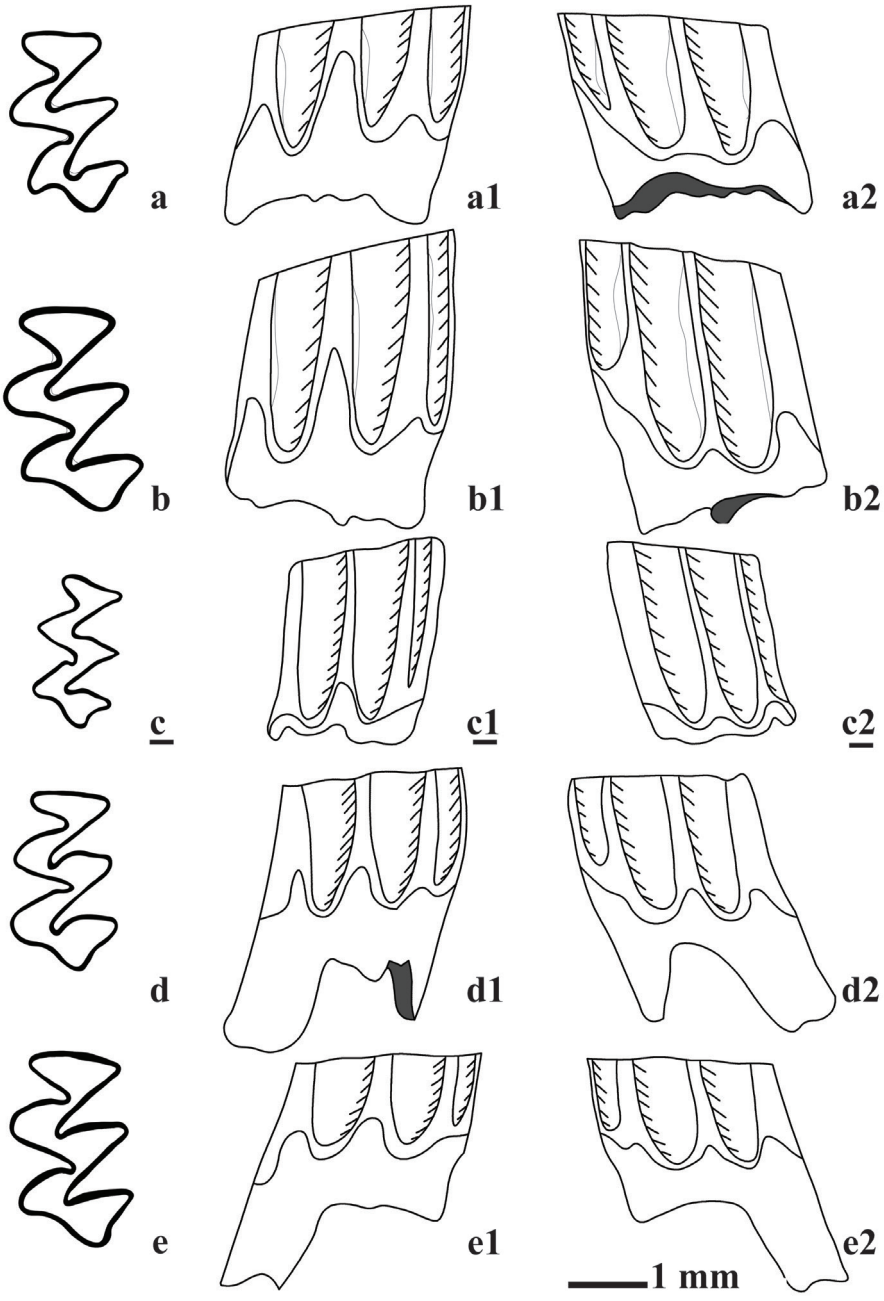

Figure 4. Arvicolinae from Afşar 2, M1: *Mimomys hassiacus*: a (PV-AFS-65), a1 (lingual view), a2 (labial view), b (PV-AFS-67), b1 (lingual view), b2 (labial view). *M. gracilis*: c (PV-AFS-135), c1 (lingual view), c2 (labial view). *Pliomys graecus*: d (PV-AFS-250), d1 (lingual view), d2 (labial view), e (PV-AFS-251), e1 (lingual view), e2 (labial view). Underlined letter indicates inversed figure of the specimen.

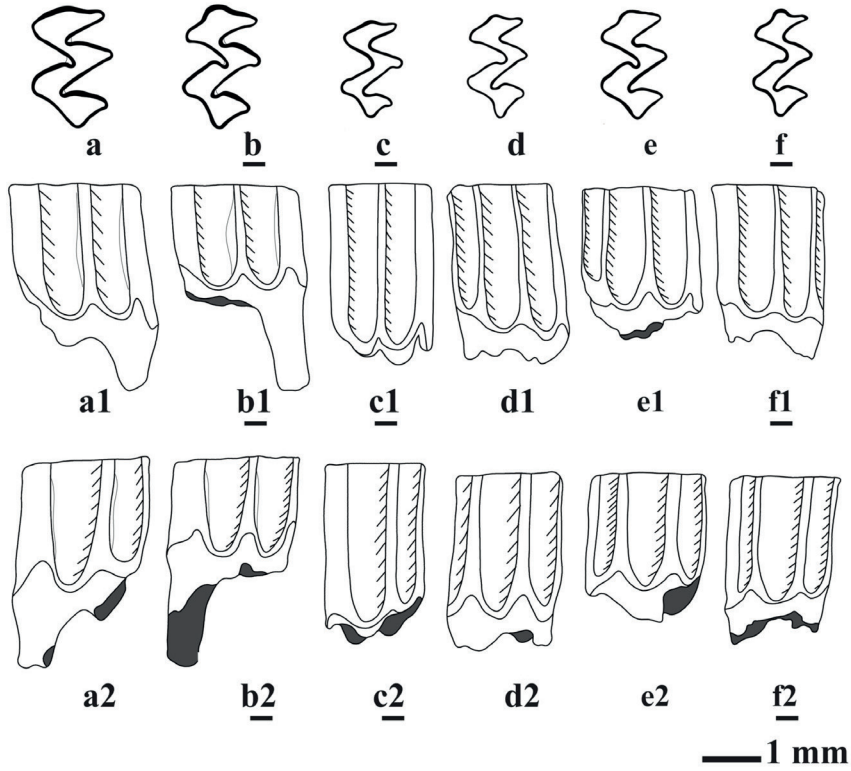

Figure 5. Arvicolinae from Afşar 2, M2: *Mimomys hassiacus*: a (PV-AFS-73), a1 (labial view), a2 (lingual view) b (PV-AFS-80), b1 (labial view), b2 (lingual view). *M. gracilis*: c (PV-AFS-141), c1 (labial view), c2 (lingual view). *Pliomys graecus*: d (PV-AFS-301), d1 (labial view), d2 (lingual view), e (PV-AFS-303), e1 (labial view), e2 (lingual view), f (PV-AFS-312), f1 (labial view), f2 (lingual view). Underlined letter indicates inversed figure of the specimen.

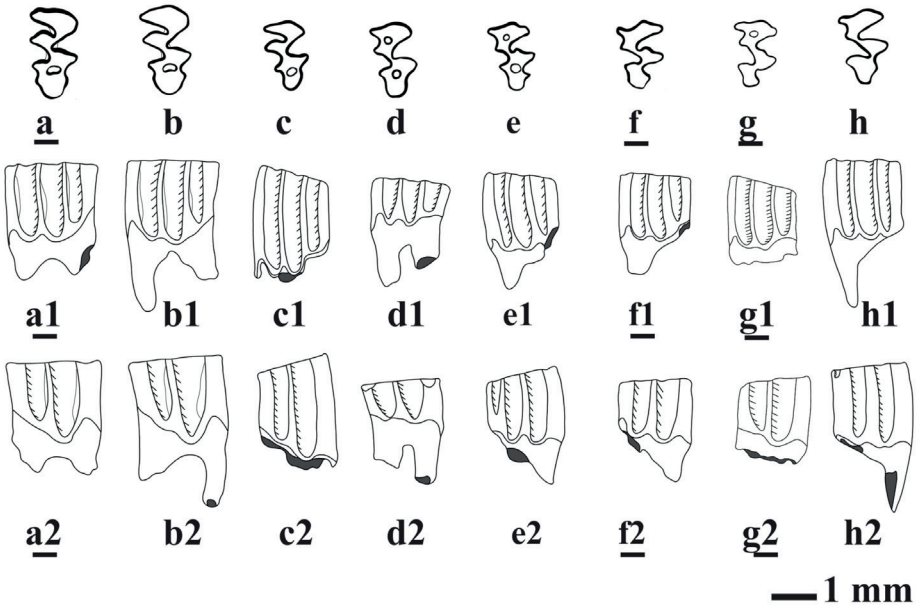

Figure 6. Arvicolinae from Afşar 2, M3: *Mimomys hassiacus*: a (PV-AFS-88), a1 (labial view), a2 (lingual view), b (PV-AFS-90), b1 (labial view), b2 (lingual view). *M. gracilis*: c (PV-AFS-146), c1 (labial view), c2 (lingual view), d (PV-AFS-147), d1 (labial view), d2 (lingual view), e (PV-AFS-148), e1 (labial view), e2 (lingual view). *Pliomys graecus*: f (PV-AFS-331), f1 (labial view), f2 (lingual view), g (PV-AFS-334), g1 (labial view), g2 (lingual view), h (PV-AFS-336), h1 (labial view), h2 (lingual view). Underlined letter indicates inversed figure of the specimen.

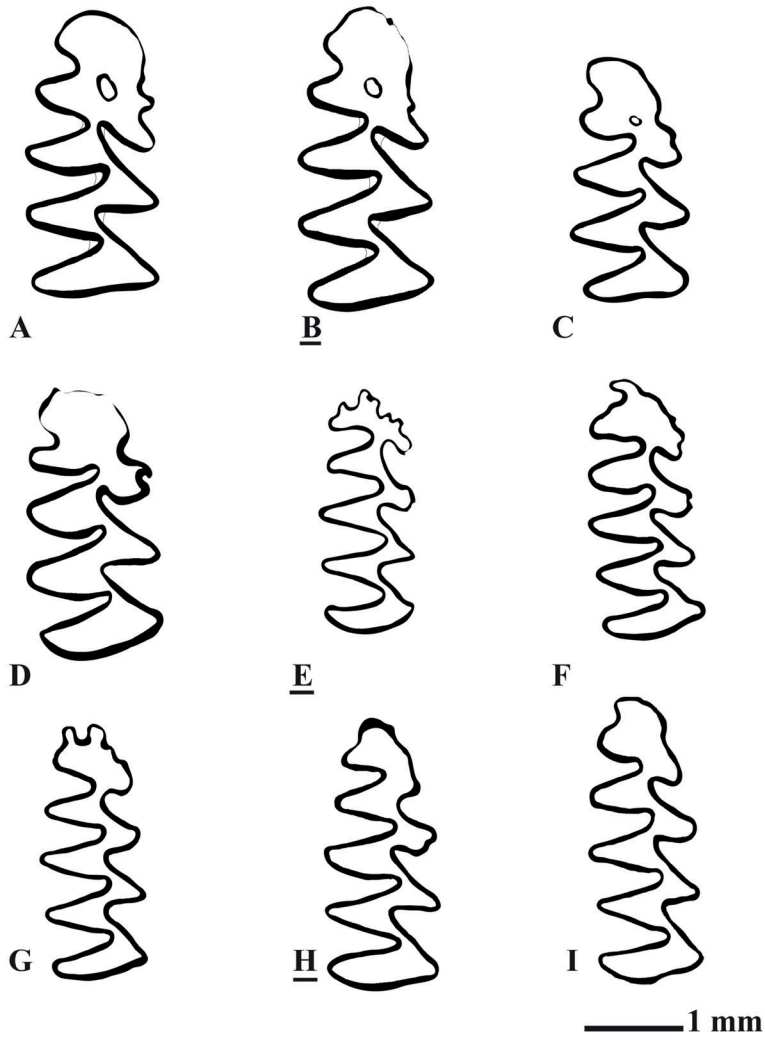

Figure 7. Arvicolinae from Afşar 2, m1, occlusal view: *Mimomys hassiacus*: a (PV-AFS-31), b (PV-AFS-36). *M. gracilis*: c (PV-AFS-94), d (PV-AFS-95). *Pliomys graecus*: e (PV-AFS-150), f (PV-AFS-156), g (PV-AFS-161), h (PV-AFS-174), i (PV-AFS-182). Underlined letter indicates inversed figure of the specimen.

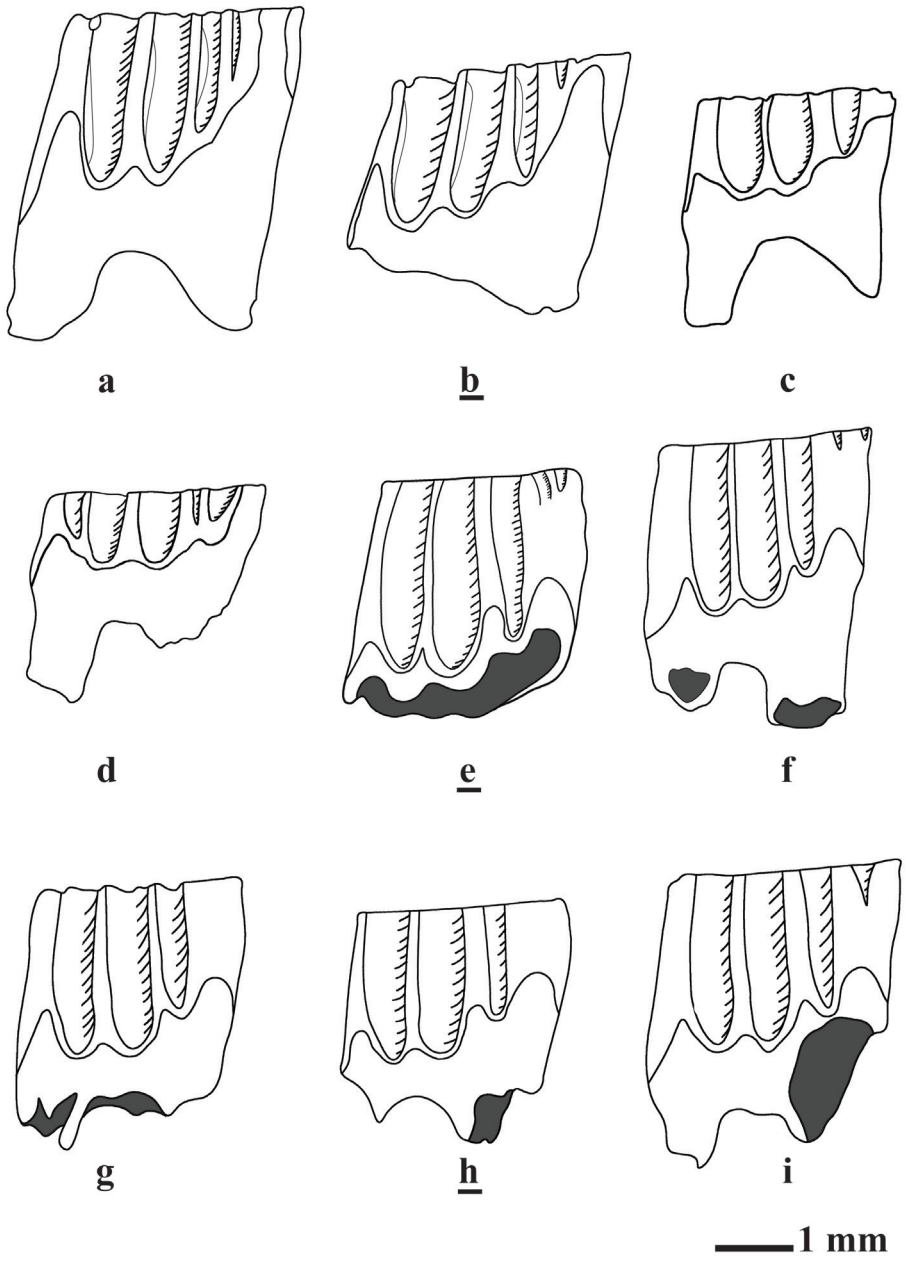

Figure 8. Arvicolinae from Afşar 2, m1, labial view: *Mimomys hassiacus*: a (PV-AFS-31), b (PV-AFS-36). *M. gracilis*: c (PV-AFS-94), d (PV-AFS-95). *Pliomys graecus*: e (PV-AFS-150), f (PV-AFS-156), g (PV-AFS-161), h (PV- AFS-174), i (PV-AFS-182). Underlined letter indicates inversed figure of the specimen.

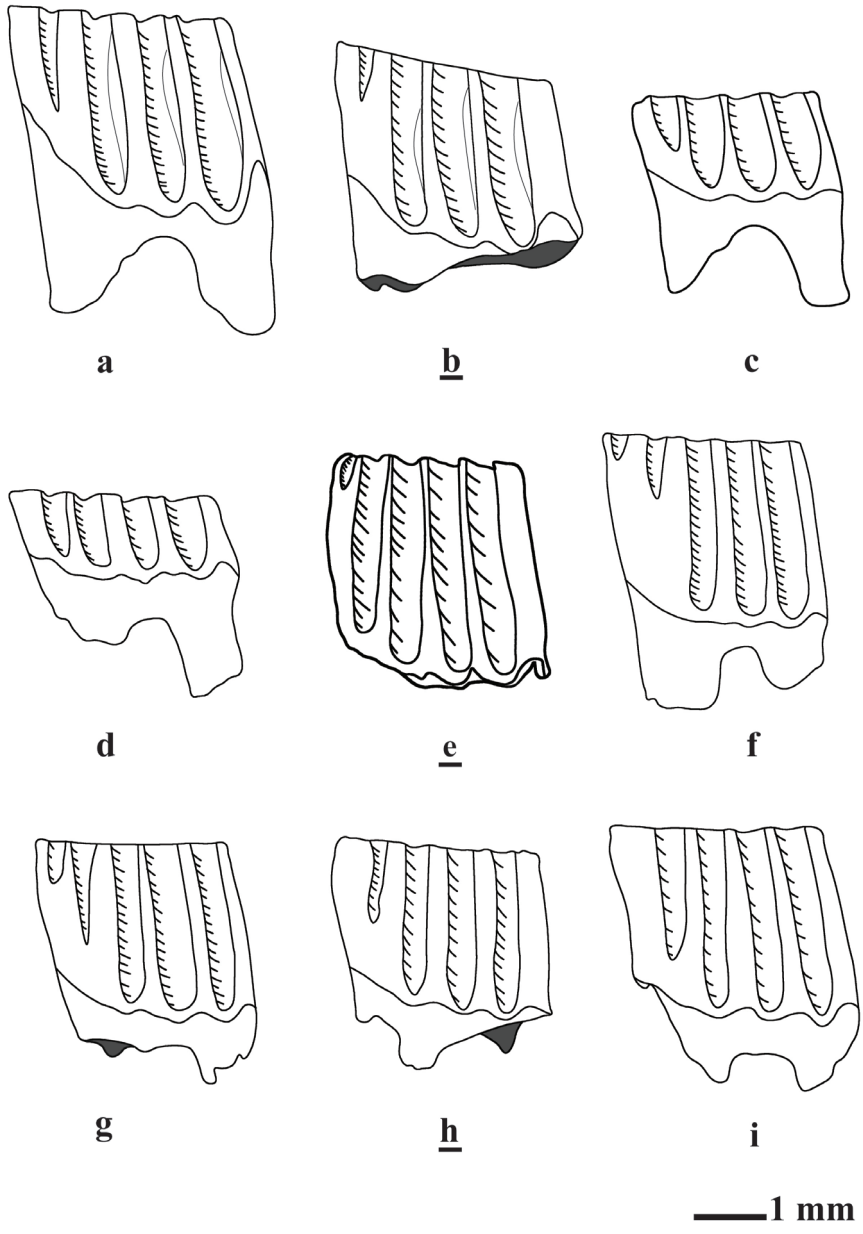

Figure 9. Arvicolinae from Afşar 2, m1, lingual view: *Mimomys hassiacus*: a (PV-AFS-31), b (PV-AFS-36). *M. gracilis*: c (PV-AFS-94), d (PV-AFS-95). *Pliomys graecus*: e (PV-AFS-150), f (PV-AFS-156), g (PV-AFS-161), h (PV- AFS-174), i (PV-AFS-182). Underlined letter indicates inversed figure of the specimen.

M2s (Figures 5a and 5b) are square-shaped molars with three roots. In six out of ten specimens, the two posterior roots are merged into one; the roots are separated in the remaining four. In the occlusal view, the molar incorporates the anterior lobe (including T1), two wide triangles (T2 and T3) and the metacone as the fourth triangle. The enamel differentiation is of the *Mimomys*-type. Inside the synclines, cement is present. The linea sinuosa is low, with the maximum height for the anterosinus of 0.71 mm and for the protosinus 0.83 mm.

M3s (Figures 6a and 6b) are the smallest of the upper molars. It has a double anterior and a smaller posterior root. Its crown comprises the protocone, the anterocone, two triangles, the metacone, and the posterior lobe. The young specimens have a deep Sl3, connected to the enamel islet, which becomes isolated in the worn specimens. The islet is well developed, but it disappears when the level of attrition is high. The enamel differentiation is of the *Mimomys* type and cement is present. The enamel-free areas are closed and relatively low. The maximum values of the anterosinus and the protosinus are 0.57 mm and 0.44 mm, respectively.

m1s (Figures 7a and 7b; 9a and 9b) are elongated and have two roots. The occlusal surface includes the posterior loop, three triangles, and the anteroconid complex; the latter contains two additional triangles and the enamel islet, which disappears in the worn specimens. The *Mimomys*-ridge is well developed but short and tends to disappear with advanced wear. The triangles are wide and confluent but the connection of the T1 with the T2 is wider than the rest. The triangles on the lingual side of the molar are vertically developed compared to the triangles on the buccal side, which are posteriorly inclined. The enamel differentiation is negative (*Mimomys* type) and the cement in the synclines is irregular. When the cement is not preserved, its mark is visible. The hyposinuid and the hyposinulid are short with the maximum value of the first being 1.09 mm and the second 0.77 mm. The anterosinuid has a vertical and acute shape. It is the highest enamel-free area with a minimum of 2.21 mm.

m2s (Figures 10a and 10b) have a posteriorly and anteriorly compressed shape and two roots. Its occlusal surface is composed by the posterior loop and four triangles. T1 and T3 are wider and longer than the other two. The enamel is not differentiated and cement is present between the triangles. Both the labial and the lingual enamel-free areas are relatively low and closed. The hyposinuid has a maximum value of 0.97 mm and the hyposinulid 0.63mm.

m3s (Figures 11a–11c) have an elongated shape with two roots. The triangles are confluent. T1 and T2 as well as T3 and T4, widely communicate to each other. The enamel differentiation tends to be negative, mostly in worn specimens, and cement is present. The highest values of the hyposinuid and the hyposinulid are 0.45 mm and 0.42 mm, respectively.

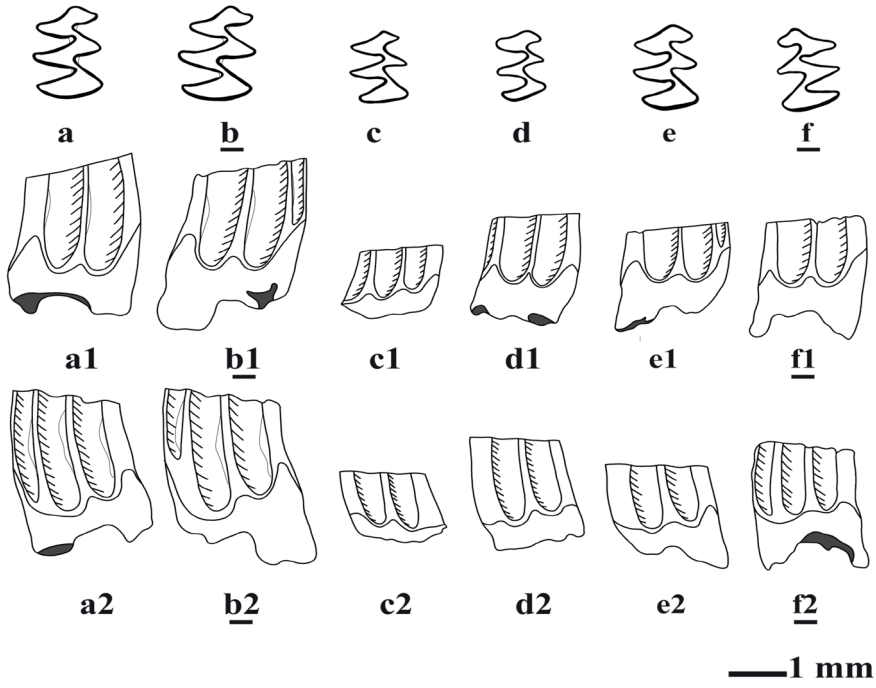

Figure 10. Arvicolinae from Afşar 2, m2: *Mimomys hassiacus*: a (PV-AFS-48), a1 (labial view), a2 (lingual view), b (PV-AFS-53), b1 (labial view), b2 (lingual view). *M. gracilis*: c (PV-AFS-101), c1 (labial view), c2 (lingual view), d (PV-AFS-104), d1 (labial view), d2 (lingual view). *Pliomys graecus*: e (PV-AFS-197), e1 (labial view), e2 (lingual view), f (PV-AFS-200), f1 (labial view), f2 (lingual view). Underlined letter indicates inversed figure of the specimen.

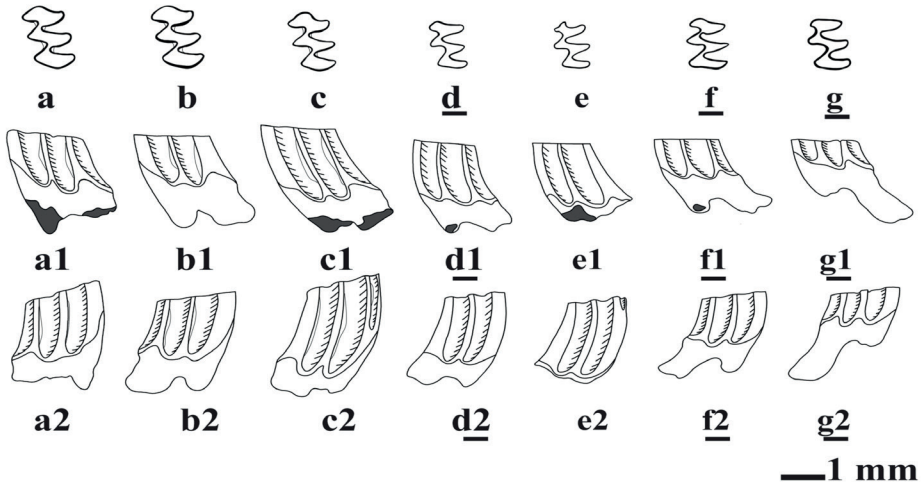

Figure 11. Arvicolinae from Afşar 2, m3: *Mimomys hassiacus*: a (PV-AFS-57), a1 (labial view), a2 (lingual view), b (PV-AFS-58), b1 (labial view), b2 (lingual view), c (PV-AFS-62), c1 (labial view), c2 (lingual view). *M. gracilis*: d (PV-AFS-109), d1 (labial view), d2 (lingual view), e (PV-AFS-117), e1 (labial view), e2 (lingual view). *Pliomys graecus*: f (PV-AFS-237), f1 (labial view), f2 (lingual view), g (PV-AFS-238), g1 (labial view), g2 (lingual view). Underlined letter indicates inversed figure of the specimen.

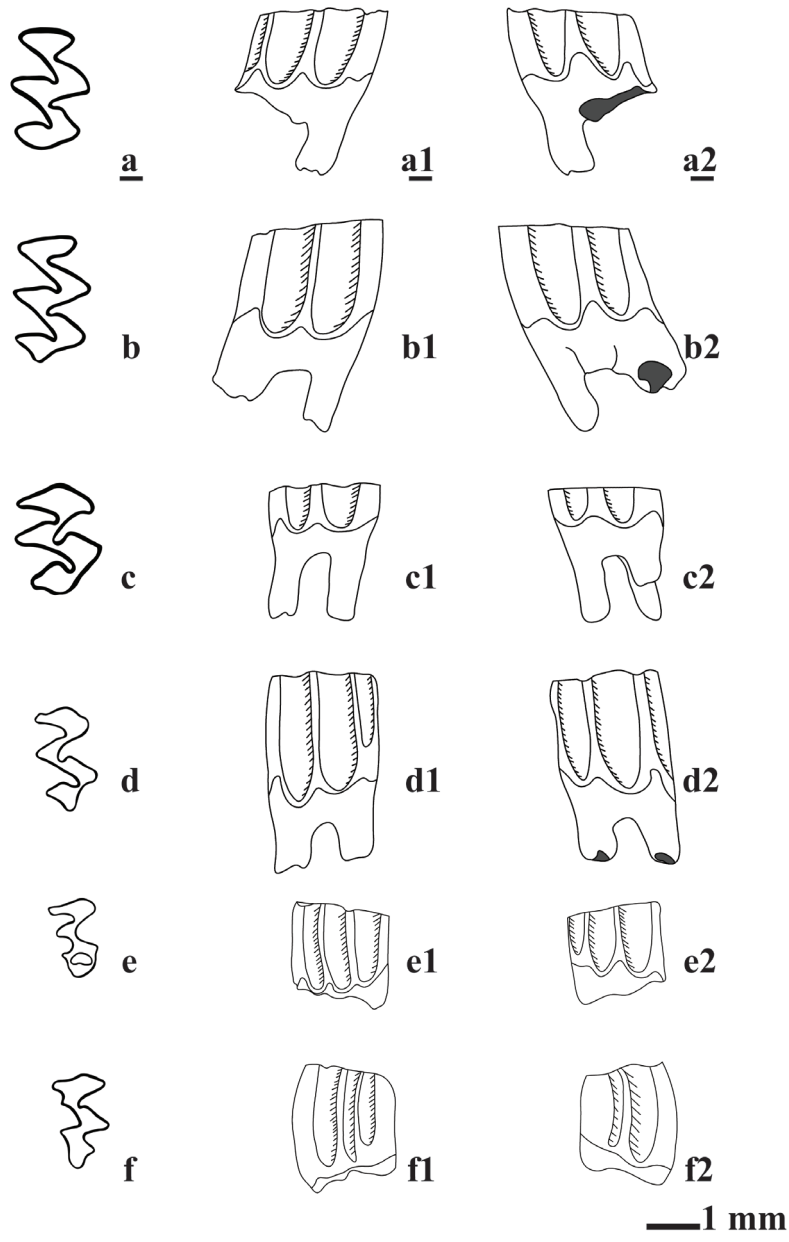

Figure 12. Arvicolinae from Afşar 1. *Pliomys* sp.: a (M1, occlusal, PV-AFS-394), a1 (labial view), a2 (lingual view), b (M1, PV-AFS-395), b1 (labial view), b2 (lingual view), c (M2, PV-AFS-401), c1 (labial view), c2 (lingual view), d (M2, PV-AFS-402), d1 (labial view), d2 (lingual view), f (M3, PV-AFS-406), f1 (labial view), f2 (lingual view); *Mimomys* cf. *gracilis*: e (M3, PV-AFS-415), e1(labial view), e2 (lingual view). Underlined letter indicates inversed figure of the specimen.

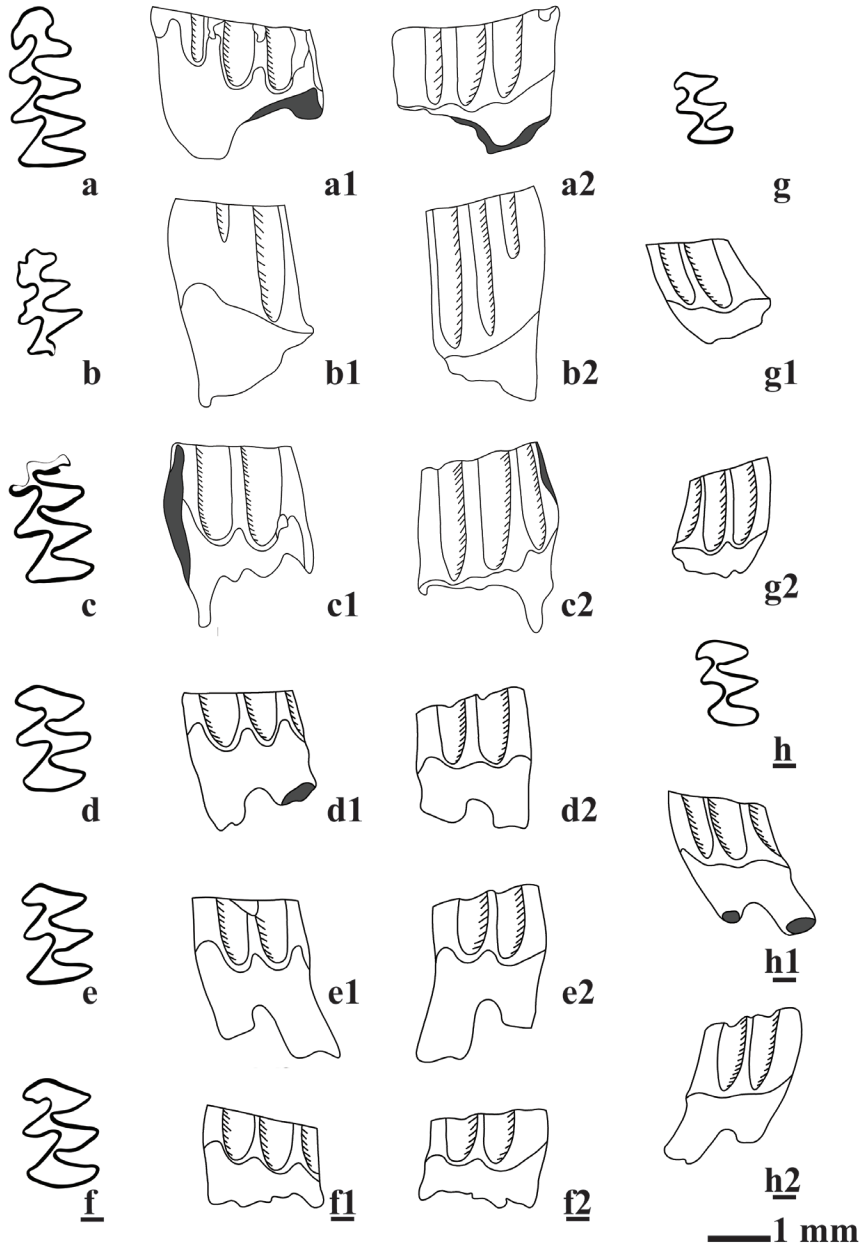

Figure 13. Arvicolinae from Afşar 1. *Pliomys* sp.: a (m1, PV-AFS-375), a1 (labial view), a2 (lingual view), e (m2, PV-AFS-377), e1 (labial view), e2 (lingual view), f (m2, PV-AFS-379), f1 (labial view), f2 (lingual view), h (m3, PV-AFS-391), h1 (labial view), h2 (lingual view); *Mimomys* cf. *gracilis*: b (m1, PV-AFS-408), b1 (labial view), b2 (lingual view), d (m2, Occlusal view, PV-AFS-410), d1 (labial view), d2 (lingual view), g (m3, PV-AFS-412), g1 (labial view), g2 (lingual view); Arvicolinae gen. Sp.: c (m1, PV-AFS-417), c1 (labial view), c2 (lingual view). Underlined letter indicates inversed figure of the specimen.

Remarks. This is the largest arvicoline in Afşar 2. The well-developed *Mimomys*-ridge and enamel islet in the m1, in addition to the negative enamel differentiation of the molars, indicate that the species belongs to *Mimomys*. Its molars are larger than those of *M. gracilis*, *M. stehlini*, and *M. davakosi* from Tomea Eksi (Hordijk and De Bruijn, 2009). On the other hand, their size is similar to *M. davakosi* from Vorio 3 (Hordijk and De Bruijn, 2009), *M. hajnackensis* from Nagavskaya, Shirokino (Tesakov, 2004: tables 4.2, 4.3) and *M. hassiacus* from the type locality of Gundersheim-1 (Heller, 1936), Hajnáčka (Fejfar, 1961), Wölfersheim (Fejfar and Repenning, 1998; Dahlmann, 2001) and Měňany 3 (Čermák et al., 2007). Finally, they are smaller than *M. hassiacus* from Tollo de Chiclana-1B (Minwer-Barakat et al., 2004; 2008) and Hambach (Mörs et al., 1998: figure 19, table 1) and *M. polonicus* from Kushkuna (Tesakov, 2004). The enamel-free areas are low and similar to those of *M. hassiacus* and *M. stehlini*. However, plotting the HH-index vs the length of the molars, we see that the *Mimomys* species from Afşar 2 is situated in the same group as the former (Figure 20). Therefore, and also because of the presence of cement in its synclines, it will be referred to as *M. hassiacus*.

Mimomys hassiacus Heller, 1936 (MN 16), *M. hajnackensis* Fejfar, 1961 (MN 16), and *M. stehlini* Kormos, 1931 (MN 15 to 16), made their appearance in the Pliocene localities of Europe. Some of them were considered synonymous by some researchers, but recognised as separate species by others. The species *M. septimanus* Michaux, 1971, and *M. kretzoi* Fejfar, 1961 from Deutsch-Altenburg 9 and 20 in Austria (Rabeder, 1981), as well as the same species from Moreda in Spain (Bachelet et al., 1991), are considered junior synonyms of *M. stehlini* (type locality San Giusto at Empoli; Kormos, 1934). Fejfar and Storch (1990) synonymized *M. hajnackensis* with *M. hassiacus* based on the presence of crown cement in the molar's synclines of the latter, something that Heller (1936) did not notice on the holotype from Gundersheim-1. Tesakov (2004), however, continues to use *M. hajnackensis* since he had doubts about the homogeneity of the sample that Fejfar and Storch studied (Mayhew et al., 2008). Therefore, he considers *M. hajnackensis* a primitive member of the *M. polonicus* Kowalski, 1960 – *M. pliocaenicus* Forsyth Major, 1902 lineage (Tesakov, 2004). After consulting the type material of *M. hajnackensis*, we agree that there are doubts on the homogeneity of the sample, but the holotype fits both in morphology and measurements well with *M. hassiacus*. Therefore, we agree with Fejfar and Storch (1990) in considering *M. hajnackensis* a junior synonym of *M. hassiacus*.

Mimomys gracilis (Kretzoi, 1959)

Original reference: *Cseria gracilis* Kretzoi, 1959, p. 242

Type locality: Csarnóta 2 (Hungary)

Locality: Afşar 2

Measurements: Table 6

Table 6. Material and measurements of *Mimomys gracilis*, Afşar 2 (mm).

M1	**N**	**Min**	**Max**	**Mean**	**Std.Dev.**	**Std.error**
Length	4	1.93	2.22	2.12	0.13	0.06
Width	3	1.19	1.53	1.35	0.17	0.10
AS	5	0.34	0.44	0.38	0.04	0.02
PRS	5	0.38	0.80	0.55	0.17	0.08
PA- index	5	0.52	0.87	0.68	0.13	0.06
M2	**N**	**Min**	**Max**	**Mean**	**Std.Dev.**	**Std.error**
Length	5	1.67	1.96	1.78	0.12	0.05
Width	5	1.05	1.41	1.20	0.15	0.07
AS	3	0.18	0.21	0.19	0.01	0.01
PRS	5	0.19	0.22	0.20	0.01	0.00
PA- index	3	0.27	0.30	0.28	0.02	0.01
M3	**N**	**Min**	**Max**	**Mean**	**Std.Dev.**	**Std.error**
Length	3	1.53	1.68	1.60	0.08	0.04
Width	3	0.98	1.06	1.02	0.04	0.02
AS	1	0.13	0.13	0.13	-	-
PRS	2	0.25	0.28	0.27	0.02	0.01
L PC	3	0.85	0.92	0.89	0.04	0.02
W PC	3	0.82	0.83	0.82	0.01	0.00
PA- index	2	0.25	0.31	0.28	0.04	0.03
LP/L	3	52.61	58.30	55.36	2.85	1.64
m1	**N**	**Min**	**Max**	**Mean**	**Std.Dev.**	**Std.error**
Length	2	2.46	2.73	2.59	0.18	0.13
Width	3	1.10	1.52	1.26	0.23	0.13
ASD	1	1.01	1.01	1.01	-	-
HSD	5	0.31	0.43	0.37	0.05	0.02
HSLD	4	0.24	0.43	0.31	0.09	0.04
AL	2	35.30	40.63	37.96	3.76	2.66
HH- index	3	0.42	0.54	0.48	0.06	0.03

Table 6. Continued

m2	N	Min	Max	Mean	Std.Dev.	Std.error
Length	8	1.34	1.60	1.47	0.08	0.03
Width	8	0.86	1.19	1.03	0.10	0.03
HSD	8	0.14	0.42	0.26	0.11	0.04
HSLD	9	0.08	0.34	0.21	0.08	0.03
HH- index	8	0.16	0.48	0.34	0.11	0.04
m3	**N**	**Min**	**Max**	**Mean**	**Std.Dev.**	**Std.error**
Length	20	1.19	1.43	1.31	0.07	0.01
Width	20	0.75	1.03	0.89	0.07	0.02
HSD	19	0.12	0.39	0.24	0.08	0.02
HSLD	22	0.08	0.34	0.19	0.07	0.02
HH- index	19	0.13	0.52	0.30	0.10	0.02

Description. M1 (Figure 4c) has an elongated outline and three roots. Its occlusal surface is composed of the anterior lobe and four broad triangles. None of them is isolated, with the connection between the T3 and T4 being the widest. The vertices of the triangles are rounded and the enamel maintains the same width. Worn specimens, however, tend towards a *Mimomys* type enamel differentiation. The cement is absent and the enamel-free areas are short and closed. The anterosinus' maximum value is 0.44 mm and the protosinus 0.80 mm high.

M2 (Figure 5c) is elongated with two roots. Its occlusal surface is confluent and the buccal and the lingual triangles have a similar size. The enamel keeps the same thickness around the triangles and the cement is absent between the synclines. The enamel-free areas are short and closed with the maximum value of the anterosinus being 0.21 mm and the protosinus 0.22 mm high.

M3s (Figures 6c–6e) have a triangular shape and two roots. Its crown is well developed, including the protocone, the anterocone, the triangles T2 and T3, the metacone and the posterior cap. The last two are almost symmetrical. The posterior enamel islet has a round shape. Two out of the three specimens have an additional anterior enamel islet. The islet of the third one is not formed yet due the level of the attrition. The enamel differentiation follows the *Mimomys* type, but its detection is difficult. The cement is absent and the enamel-free areas are relatively low and closed. The anterosinus height does not surpass the 0.13 mm with the maximum value of the protosinus being 0.28 mm.

The m1 (Figures 7c and 7d; 9c and 9d) molars are elongated with two roots. The crown is composed of the posterior lobe and five triangles. The T4 and T5, as well as the round enamel islet and the underdeveloped *Mimomys*- ridge, form the anteroconid complex. The enamel differentiation tends to be negative (*Mimomys* type) and the cement is absent. The enamel-free areas are closed and very low.

The maximum value of the hyposinuid and the hyposinulid is 0.43 mm. The anterosinuid was able to be measured in one of the five molars, with its value being 1.01 mm.

m2s (Figures 10c and 10d) has an anteriorly and posteriorly compressed shape and two parallel developed roots. Its occlusal surface is slightly confluent and composed by the posterior lobe and four triangles. The lingual triangles are perpendicular to the length axis and more elongated than the labial ones. T4 is the smallest of the triangles. The enamel has the same width throughout and the cement is absent. The enamel-free areas are short with the maximum value of the hyposinuid and the hyposinulid being 0.42 mm and 0.34, respectively.

m3s (Figures 11d and 11e) are elongated molars with two roots. It consists of the posterior lobe and four triangles. T1 and T3 are the most elongated ones and T4 is the smallest and hardly distinguishable in some worn specimens. All triangles are perpendicular to the length axis of the molar. The occlusal surface of the molar is confluent and the connection between the T1 and T2 is the widest. The cement is absent and the enamel width is similar around the triangles. The enamel-free areas are short. The hyposinuid does not surpass the 0.39 mm and the hyposinulid the 0.34 mm.

Remarks. This is the smallest arvicoline in Afşar. The low enamel-free areas, the size of the molar, and the almost undifferentiated enamel are typical for Early Pliocene Arvicolinae. In addition, the negative enamel differentiation observed in the worn molars, the number of the triangles, the development of the *Mimomys*-ridge and the enamel islet indicate a *Mimomys* species. This species has a size similar to those of *M. gracilis* from Csarnóta 2 (Kretzoi, 1959; Michaux, 1971), Escorihuela A (Mein et al., 1990), Wölfersheim (Fejfar and Repenning, 1998; Dahlmann, 2001), Nimes and Węże (Michaux, 1971), and to *M. cf. gracilis* from Zverinogolovskoye (Pogodina and Strukova, 2016). However, our finds are more elongated than those from Escorihuela A. Its size is smaller than

M. occitanus from the type locality of Sète (Thaler, 1955) and from Muselievo (Popov, 2004). Its occlusal surface is morphologically similar to *M. occitanus* and *M. hassiacus*; the linea sinuosa is similar to the first. However, its small size, the lack of the cement and the low enamel-free areas cause us to assign our specimens to *Mimomys gracilis*. Kretzoi (1959) described *M. gracilis*, from the Hungarian locality of Csarnóta, as *Cseria gracilis* Kretzoi, 1959. However, Kowalski (1960), Fejfar et al. (1998), and Hordijk and De Bruijn (2009) consider *Cseria* Kretzoi, 1959 as a younger synonym of *Mimomys*. Furthermore, Ruiz Bustos and Sesé (1985) and Ruiz Bustos (1987) proposed the synonymization of *M. stehlini*, *M. occitanus*, *M. gracilis*, *M. polonicus*, and *M. hassiacus*. We do not agree with this latter suggestion since the mentioned species are morphologically different. In addition, these authors did not take into account the diagnostic height of the enamel- free areas.

Mimomys cf. *gracilis* (Kretzoi, 1959)
Type locality: Csarnóta 2 (Hungary)
Locality: Afşar 1
Measurements: Table 7

Table 7. Material and measurements of *Mimomys* cf. *gracilis*, Afşar 1 (mm).

M2	**N**	**Min**	**Max**	**Mean**	**Std.Dev.**	**Std.error**
Length	1	-	-	2.02	-	-
Width	1	-	-	1.43	-	-
AS	-	-	-	-	-	-
PRS	1	-	-	0.25	-	-
PA- index	-	-	-	-	-	-
M3	**N**	**Min**	**Max**	**Mean**	**Std.Dev.**	**Std.error**
Length	1	-	-	1.41	-	-
Width	1	-	-	1.07	-	-
AS	-	-	-	-	-	-
PRS	-	-	-	-	-	-
L PC	1	-	-	0.73	-	-
W PC	1	-	-	0.85	-	-
PA- index	-	-	-	-	-	-
LP/L	1	-	-	52.13	-	-
m2	**N**	**Min**	**Max**	**Mean**	**Std.Dev.**	**Std.error**
Length	1	-	-	1.81	-	-
Width	1	-	-	1.30	-	-
HSD	1	-	-	0.26	-	-
HSLD	1	-	-	0.24	-	-
HH- index	1	-	-	0.35	-	-
m3	**N**	**Min**	**Max**	**Mean**	**Std.Dev.**	**Std.error**
Length	2	1.33	1.34	1.33	0.01	0.01
Width	2	0.87	0.89	0.88	0.02	0.01
HSD	2	0.11	0.31	0.21	0.14	0.10
HSLD	2	0.10	0.23	0.17	0.09	0.07
HH- index	2	0.15	0.39	0.27	0.17	0.12

M2 has an elongated outline. Its roots are broken. The enamel surface of the triangles is confluent. The anterior lobe, the triangles T2, T3, and T4 are alternating and similar in size. The cement is absent and enamel differentiation follows the *Mimomys* type. The enamel-free areas are low; the maximum height of the protosinus is 0.25 mm.

M3 (Figure 12e) has a triangle shape. Its roots are broken. Its occlusal surface is confluent including the anterior lobe, the triangles T2 and T3, the metacone and the posterior cap. T3 is placed opposite the metacone. The posterior enamel islet is wide and perpendicular to the length axis of the molar. The anterior islet is present deeper in the Sb1 syncline. The cement is absent and the linea sinuosa low.

The single m1 (Figure 13b) molar is broken posteriorly. It preserves its anterior wide root. It is a young specimen and its anterior cap is decorated with additional ridges. The occlusal surfaces of the triangles are confluent. The triangles are perpendicular to the length axis of the molar and the labial ones are smaller than the lingual. The *Mimomys*-ridge is well developed and the enamel island is present in the lower parts of the molar. The enamel differentiation cannot be observed due to the wear stage and the cement is absent.

m2 (Figure 13d) is anteriorly and posteriorly compressed. It has two roots; the posterior one is wider than the anterior one. Only the connection between T1 and T2 is wide. The triangles are perpendicular to the length axis of the molar and have a similar size. The cement is absent and enamel is not differentiated. The enamel-free areas are low. The maximum value of the hyposinuid is 0.26 mm and that of the hyposinulid 0.24 mm.

m3 (Figure 13g) is the smallest of the molars. Its occlusal surface incorporates the posterior lobe and four triangles. The lingual triangles are wider and more elongated than the lingual. All of them are perpendicular to the length axis of the molar. Other than the connection between T1 and T2, the rest of the dentine surfaces are connected through a narrow field. The cement is absent and the enamel is undifferentiated. The enamel-free areas are low with the maximum value of hyposinuid being 0.31 mm and the hyposinulid 0.23 mm.

Remarks. The lack of the cement, the height of the enamel-free areas, the undifferentiated enamel, the enamel islet in the m1 and the wide posterior islet of the M3 molar, indicate an Early Pliocene *Mimomys* species. The molars from Afşar 1 resemble those of *M. occitanus* from the locality of Ericek in Turkey (Hoek Ostende et al., 2015). However, they are smaller than *M. occitanus* and similar in size to *M. gracilis* from Escorihuela A, in Spain (Mein et al., 1990; Figure 20). The broken single m1 molar prohibits the measurement of the posterior enamel-free areas, which is essential to determine the height of the molar. Therefore, and especially because of its small size, the species is assigned to *M.* cf. *gracilis*.

Genus *Pliomys* Méhely, 1914

Pliomys graecus De Bruijn and Van der Meulen, 1975

Type locality: Tourkobounia-1 (Greece)

Locality: Afşar 2

Measurements: Table 8

Table 8. Material and measurements of *Pliomys graecus*, Afşar 2 (mm).

M1	**N**	**Min**	**Max**	**Mean**	**Std.Dev.**	**Std.error**
Length	31	1.95	2.45	2.29	0.11	0.02
Width	30	0.92	1.66	1.44	0.14	0.03
AS	27	0.21	0.85	0.37	0.11	0.02
PRS	29	0.24	0.68	0.41	0.11	0.02
PA- index	22	0.40	0.75	0.53	0.10	0.02
M2	**N**	**Min**	**Max**	**Mean**	**Std.Dev.**	**Std.error**
Length	29	1.75	2.10	1.92	0.09	0.02
Width	26	1.08	1.49	1.33	0.10	0.02
AS	26	0.18	0.44	0.29	0.07	0.01
PRS	23	0.18	0.39	0.28	0.06	0.01
PA- index	21	0.25	0.55	0.40	0.08	0.02
M3	**N**	**Min**	**Max**	**Mean**	**Std.Dev.**	**Std.error**
Length	25	1.40	1.83	1.64	0.10	0.02
Width	24	0.97	1.25	1.10	0.08	0.02
AS	12	0.10	0.30	0.20	0.06	0.02
PRS	13	0.10	0.34	0.22	0.08	0.02
L PC	26	0.80	1.15	0.98	0.09	0.02
W PC	24	0.69	1.00	0.88	0.07	0.01
PA- index	13	0.15	0.43	0.28	0.09	0.02
LP/L	25	51.18	65.81	59.83	3.63	0.73
m1	**N**	**Min**	**Max**	**Mean**	**Std.Dev.**	**Std.error**
Length	18	2.53	2.92	2.73	0.10	0.02
Width	19	1.05	1.36	1.19	0.08	0.02
ASD	14	0.71	1.28	1.01	0.17	0.04
HSD	22	0.50	0.75	0.62	0.07	0.02
HSLD	21	0.24	0.63	0.40	0.09	0.02
AL	17	38.03	52.71	46.11	4.62	1.12
HH- index	19	0.58	0.95	0.74	0.09	0.02

Table 8. Continued

m2	N	Min	Max	Mean	Std.Dev.	Std.error
Length	33	1.54	1.92	1.71	0.08	0.01
Width	32	1.00	1.43	1.24	0.09	0.02
HSD	28	0.26	0.70	0.48	0.10	0.02
HSLD	28	0.21	0.51	0.33	0.08	0.02
HH- index	23	0.24	0.76	0.58	0.13	0.03
m3	**N**	**Min**	**Max**	**Mean**	**Std.Dev.**	**Std.error**
Length	15	1.46	1.59	1.51	0.04	0.01
Width	13	0.80	1.12	1.00	0.09	0.02
HSD	15	0.13	0.36	0.22	0.06	0.01
HSLD	13	0.08	0.31	0.18	0.06	0.02
HH- index	12	0.19	0.47	0.29	0.08	0.02

Description. M1s (Figures 4d and 4e) have three roots. The anterior lobe is narrower than T1 and T2; the latter has the widest dentine field. Other than the connection between the T3 and T4, the triangles' communication is narrow. Enamel is not differentiated and cement is absent. The enamel-free areas are relatively low with the highest of them being the protosinus. The maximum height of the latter is 0.68 mm while that of the anterosinus is 0.85 mm.

M2s (Figures 5d–5f) have elongated shape but are also compressed on the anterior and posterior side of the molar. It has three well-developed roots, one in the anterior side and two connected ones posteriorly. The dentine fields of the triangles communicate with narrow connections that tend to become wider with wear. Three of the 32 specimens (PV-AFS-300, PV-AFS-303, PV-AFS-315) have an additional syncline on the anterior side of the molar, next to the protosinus. The enamel is not differentiated and the cement is absent. The linea sinuosa is low and the enamel-free areas closed. The maximum height of the protosinus and the anterosinus are 0.43 mm and 0.44 mm, respectively.

M3s (Figures 6f–6h) have a triangle shape with the anterior part being wider than the posterior. It has two roots and its occlusal surface comprises the anterior lobe (including the protocone and the anterocone), two additional triangles (T2 and T3), the metacone, and the posterior lobe. The latter is almost isolated from the rest of the molar and it includes an additional small T4. Three out of the 31 molars have an anterior enamel islet and only one (PV-AFS-340) maintains an anterior one due to the T3 and T4 fusion. The enamel maintains the same width and the cement is absent. The maximum value of the protosinus is 0.34 mm while that of the anterosinus does not exceed 0.30 mm.

m1s (Figures 7e–7i and 9e–9i) are elongated with a wide anterior and a smaller posterior root. Its lingual triangles are much longer and wider than the labial ones. In addition, they are perpendicular to the length axis of the molar with the labial being posteriorly oriented. T4 has an almost square shape and T6 and

T7 are notably distinct. The occlusal dentine fields communicate with narrow connections and enamel is undifferentiated. The cement is absent. In younger specimens, the anterior part of the anterior cap is decorated with additional ridges that tend to disappear in worn specimens. The *Mimomys*-ridge is present but almost fused into the T4. Five of the 43 specimens have an anterolingual enamel islet. The enamel- free areas are low and closed. The highest of them is the anterosinuid with a maximum value of 1.28 mm.

m2s (Figures 10e and 10f) have an elongated shape with compressed anterior and posterior outlines. The posterior of the two roots is wider than the anterior. The occlusal surface is confluent, but in worn molars, the triangles tend to become isolated. The lingual triangles are vertically developed to the molar and wider than the posteriorly inclined labial ones. The cement is absent and enamel is not differentiated. The highest values of the hyposinuid and the hyposinulid are 0.70 mm and 0.51 mm, respectively.

m3s (Figures 11f and 11g) have an elongated shape and two roots. The connection between the dentine fields of the occlusal view is narrow. The alternating triangles are posteriorly oriented. The lingual ones are wider and more elongated than the labial ones. The synclines lack cement and the enamel keeps the same width throughout. The highest value of the hyposinuid is 0.36 mm, while that of the hyposinulid is 0.31 mm.

Remarks. The most abundant rodent of Afşar closely resembles *Pliomys graecus* De Bruijn and Van der Meulen, 1975 from its type locality Tourkobounia-1, in Greece. Its size is similar to the Greek assemblage and the M3 molars have two roots and a mostly isolated posterior lobe. It differs from the type assemblage in the height of the m1 enamel- free areas, which are slightly lower than in Tourkobounia-1 and the presence of a weak *Mimomys*-ridge (Figures 7F and 7H) in young specimens. The Turkish arvicoline differs from *Pliomys hungaricus* (Kormos, 1934) in having only two-rooted M3. It is smaller than *P. hungaricus* from the type locality of Csarnóta 2 in Hungary and from Muselievo in Bulgaria (Popov, 2004), but it is similar in size to the same species from Ptolemais in Greece (Hordijk and De Bruijn, 2009). The height of the HSD is similar to *P. hungaricus* from Csarnóta (Kormos, 1934) and Muselievo (Popov, 2004), but lower than that from Ptolemais. The morphology of the anterior cap in m1, with its additional triangles T6 and T7, distinguishes this vole from the species *P. kowalskii* Schevtschenko, 1965, *P. jalpugensis* Nesin, 1983, and *P. destinatus* Tesakov, 2005. The species from Afşar differs from *P. ucrainicus* (Topachevsky and Scorik, 1967) in the rounder anterior cap of the m1 with a less vergent reentrant fold, which is anteriorly developed to T7, the mimomyoid characters like the *Mimomys*-ridge and the presence of an anterior enamel islet on the M3. The molar size, the height of the enamel-free areas, and the two-rooted M3 molars with the isolated posterior dentine fields assign our specimens to *Pliomys graecus*. However, the mimomyioid characters like the weak *Mimomys*-ridge and the slightly lower enamel-free areas indicate a more primitive representative of the species.

According to Tesakov (2005), *Pliomys graecus* from the Greek locality of Tourkobounia-1 is identical to *Pliomys ucrainicus* (Topachevsky and Scorik, 1967). *Pliomys hungaricus* (Kormos, 1934) was first described as a *Dolomys* species. Kretzoi (1959), erected the genus *Propliomys* Kretzoi, 1959 based on the uniform enamel ("gleichmässige Schmelzdicke") and the number of roots in the upper molars. De Bruijn and

Van der Meulen (1975), however, emphasised that these characters are typical in most of the primitive species. Therefore, they placed the species in *Pliomys*. Here, we follow their suggestion.

Pliomys sp.

Locality: Afşar 1

Measurements: Table 9

Table 9. Material and measurements of *Pliomys* sp., Afşar 1 (mm).

M1	**N**	**Min**	**Max**	**Mean**	**Std.Dev.**	**Std.error**
Length	4	2.10	2.31	2.20	0.10	0.05
Width	4	1.32	1.51	1.40	0.10	0.05
AS	5	0.18	0.32	0.26	0.05	0.02
PRS	6	0.26	0.46	0.39	0.08	0.03
PA- index	5	0.41	0.56	0.49	0.06	0.03
M2	**N**	**Min**	**Max**	**Mean**	**Std.Dev.**	**Std.error**
Length	2	1.92	2.03	1.97	0.08	0.06
Width	2	1.08	1.57	1.32	0.35	0.25
AS	2	0.20	0.27	0.23	0.05	0.04
PRS	2	0.21	0.31	0.26	0.07	0.05
PA- index	2	0.29	0.41	0.35	0.09	0.06
M3	**N**	**Min**	**Max**	**Mean**	**Std.Dev.**	**Std.error**
Length	1	-	-	1.67	-	-
Width	1	-	-	1.07	-	-
AS	1	-	-	0.20	-	-
PRS	1	-	-	0.25	-	-
L PC	1	-	-	1.05	-	-
W PC	1	-	-	0.88	-	-
PA- index	1	-	-	0.31	-	-
LP/L	1	-	-	62.66	-	-
m1	**N**	**Min**	**Max**	**Mean**	**Std.Dev.**	**Std.error**
Length	1	-	-	2.61	-	-
Width	1	-	-	1.36	-	-
ASD	1	-	-	0.94	-	-
HSD	-	-	-	-	-	-
HSLD	-	-	-	-	-	-
AL	1	-	-	42.73	-	-
HH- index	-	-	-	-	-	-

Table 9. Continued

m2	N	Min	Max	Mean	Std.Dev.	Std.error
Length	7	1.64	1.81	1.73	0.06	0.02
Width	7	1.14	1.37	1.25	0.09	0.03
HSD	8	0.24	0.49	0.34	0.10	0.03
HSLD	9	0.17	0.36	0.23	0.07	0.02
HH- index	7	0.31	0.61	0.42	0.11	0.04
m3	**N**	**Min**	**Max**	**Mean**	**Std.Dev.**	**Std.error**
Length	3	1.54	1.60	1.58	0.03	0.02
Width	3	0.99	1.05	1.03	0.03	0.02
HSD	3	0.09	0.36	0.20	0.14	0.08
HSLD	4	0.10	0.21	0.17	0.05	0.03
HH- index	3	0.13	0.42	0.26	0.14	0.08

Description. M1s (Figures 12a and 12b) are elongated with three long roots. None of the triangles is isolated; in worn specimens the connection between T1 and T2 is the widest. The triangles have similar size. The cement is absent and enamel is undifferentiated. The protosinus is the highest enamel-free area and it does not exceed 0.46 mm.

M2s (Figures 12c and 12d) have an elongated outline, compressed in the two edges of the molar. Both specimens have three well-divided and strong roots. The enamel surface of the triangles is confluent and tends to become wider with wear. The alternating triangles have similar size. The cement is absent and enamel is undifferentiated. The enamel-free areas are low; the maximum height of the protosinus and the anterosinus are 0.31 mm and 0.27 mm, respectively.

M3 (Figure 12, f) has an elongated but anteriorly compressed shape. The roots have not been preserved. The occlusal surface is confluent including the anterior lobe, the triangles T2 and T3, the metacone and the posterior cap. The enamel islet is absent. T2 is the widest and the more elongated triangle. The cement is absent. The enamel differentiation tends to be negative. The enamel-free areas are low. The maximum value of the protosinus is 0.25 mm while that of the anterosinus is 0.20 mm.

m1 (Figure 13a) is worn and has an elongated outline. It has a wide anterior root; the posterior one is broken. Its occlusal surface includes the posterior lobe, the triangles T1 to T3 and the anteroconid complex, which incorporates T4 to T6. None of the alternating triangles is isolated, with the lingual ones being wider and more elongated than the buccal ones. In addition, the lingual triangles are perpendicular to the length axis of the molar, while the buccal are posteriorly oriented. The reentrant folds are vergent and the enamel preserves the same width throughout. The cement is absent. The enamel-free areas are low with the anterosinuid being the highest one at 0.94 mm height.

m2s (Figures 13e and 13f) have an elongated outline
and two roots; the posterior one is wider than the anterior one. The dentine surface of the alternated triangles is confluent, but the connections are narrow. The buccal triangles are longer and more elongated than the lingual ones. The latter are posteriorly oriented. Enamel is not differentiated and cement is absent. The enamel-free areas are low. The hyposinuid does not exceed 0.49 mm and the hyposinulid 0.36 mm height.

m3 (Figure 13h) is an elongated molar with two roots. The occlusal surface of the posterior lobe and the four triangles is confluent. The connections between the posterior lobe and T1, and that of the T2 with T3, are narrow. The lingual triangles are posteriorly oriented and much larger than the buccal ones. The enamel has a similar width throughout and there is no cement in the synclines. The enamel-free areas are low; the maximum value of the hyposinuid is 0.36 mm and the hyposinulid 0.21 mm.

Remarks. The number of alternating triangles, the small labial triangles, the low enamel-free areas, the elongated posterior lobe of the M3, the absence of cement and an enamel islet indicate that we are dealing with a species referable to *Pliomys*. Its size is similar to that of *P. destinatus* from Odessa in Ukraine (Tesakov, 2005) and *P. graecus* from Afşar 2. However, the wider anterior lobe and the additional T6 triangle of the m1 also resemble the situation in *P. hungaricus* from Csarnóta in Hungary and Ptolemais in Greece. Unfortunately, the diagnostic molars m1 and M3, are both represented by one specimen only, with the m1 being highly worn. Therefore, we deem it prudent to refer this species to *Pliomys* sp.

Arvicolinae gen. sp.
Locality: Afşar 1

A single m1 molar (Figure 13c) with an anterior part broken preserves the posterior lobe and the triangles T1 to T3. The triangles are perpendicular to the length axis of the molar, having a similar size. The occlusal surface is confluent and the connections are narrow. The enamel differentiation is difficult to observe but tends to be negative. The cement is absent. The enamel-free areas are short and closed; the hyposinuid is 0.44 mm and the hyposinulid 0.19 mm height.

Remarks. The broken anterior part of the m1 molar hides important identification characters like the additional triangles, the morphology of the anteroconid complex and the enamel islet. The low enamel-free areas, lack of the cement and negative enamel differentiation suggests an Early Pliocene *Mimomys* species. The molar is larger than the corresponding teeth of the recorded *Mimomys* cf. *gracilis* and *Pliomys* sp. However, the level of wear and damage prevent the identification on a species and genus level.

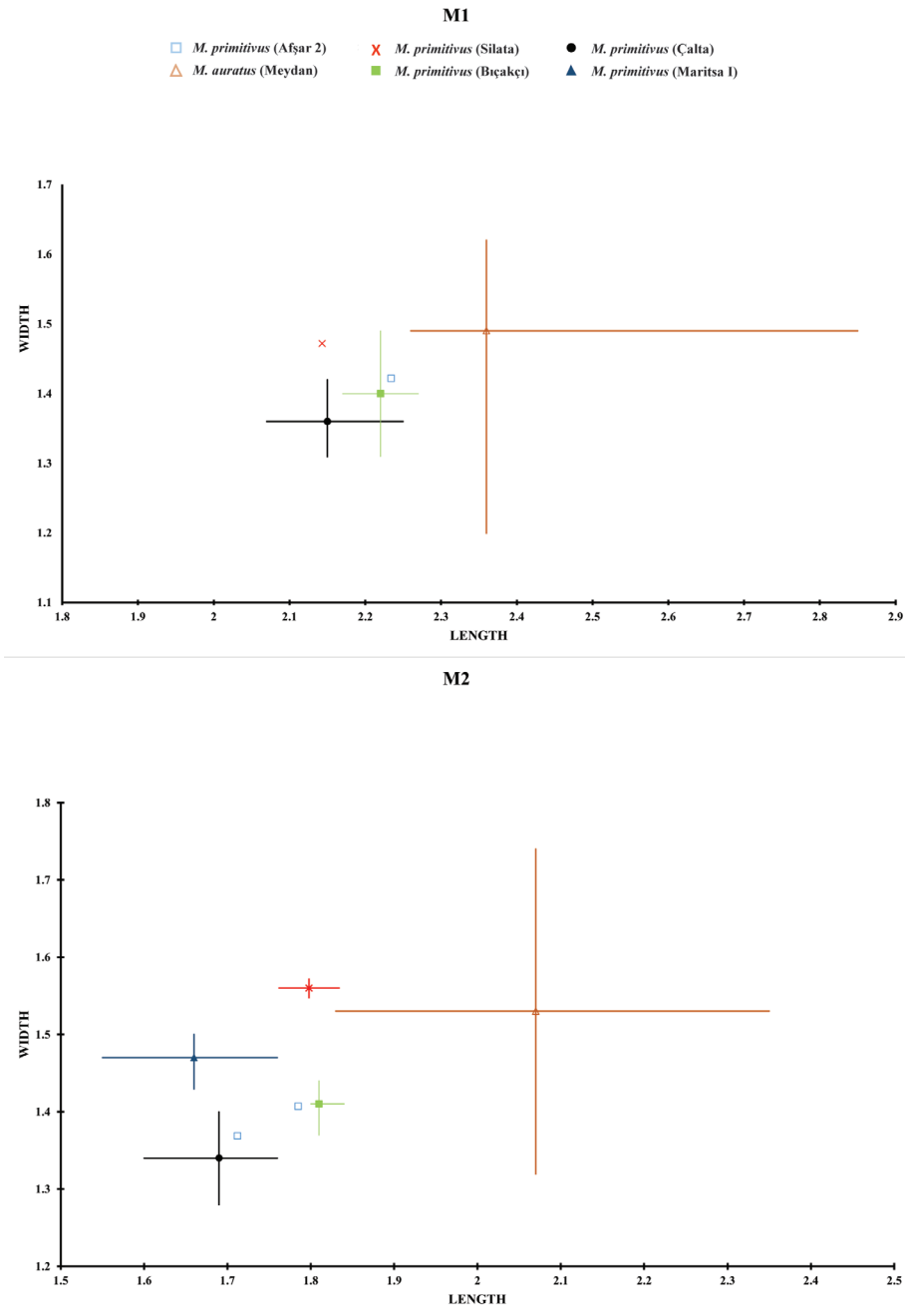

Figure 14. L/W scatter plot of the M1 and M2 molars from *Mesocricetus primitivus* from Afşar 2, Silata (MN 13/14), Çalta (MN 15), Bıçakçı (MN 17), Maritsa I (MN 15) (De Bruijn et al., 1970; Şen, 1977; Vasileiadou et al., 2003; Hoek Ostende et al., 2015); *M. auratus* from Meydan (Holocene) (Holocene) (Hír, 1992). Measurements were made in mm.

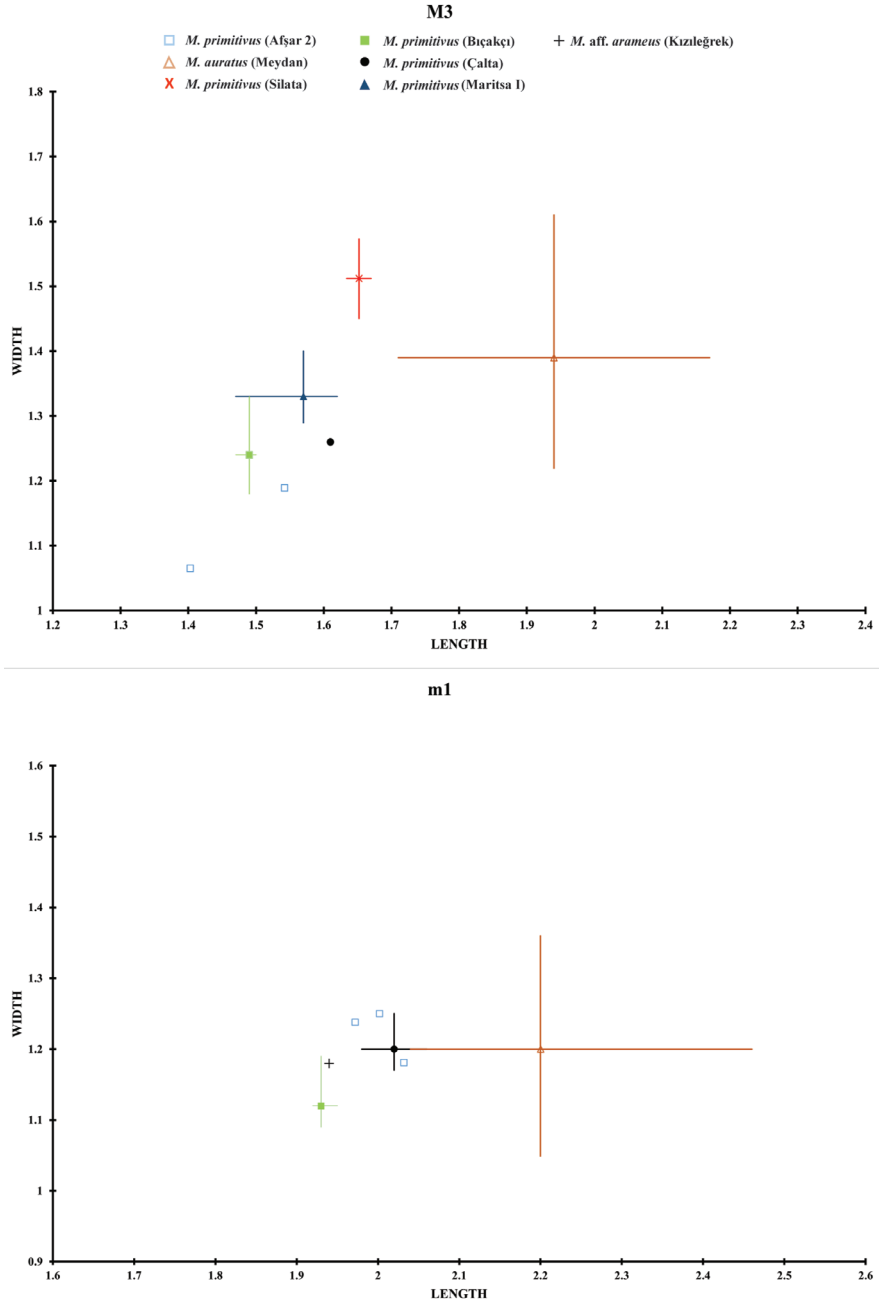

Figure 15. L/W scatter plot of the M3 and m1 from *Mesocricetus primitivus* from Afşar 2, Silata (MN 13/14), Çalta (MN 15), Bıçakçı (MN 17), Maritsa I (MN 15) (De Bruijn et al., 1970; Şen, 1977; Vasileiadou et al., 2003; Hoek Ostende et al., 2015); *M. auratus* from Meydan (Holocene) (Hír, 1992); *M.* aff. *arameus* from Kızıleğrek (Early Biharian) (Erturaç et al., 2019). Measurements were made in mm.

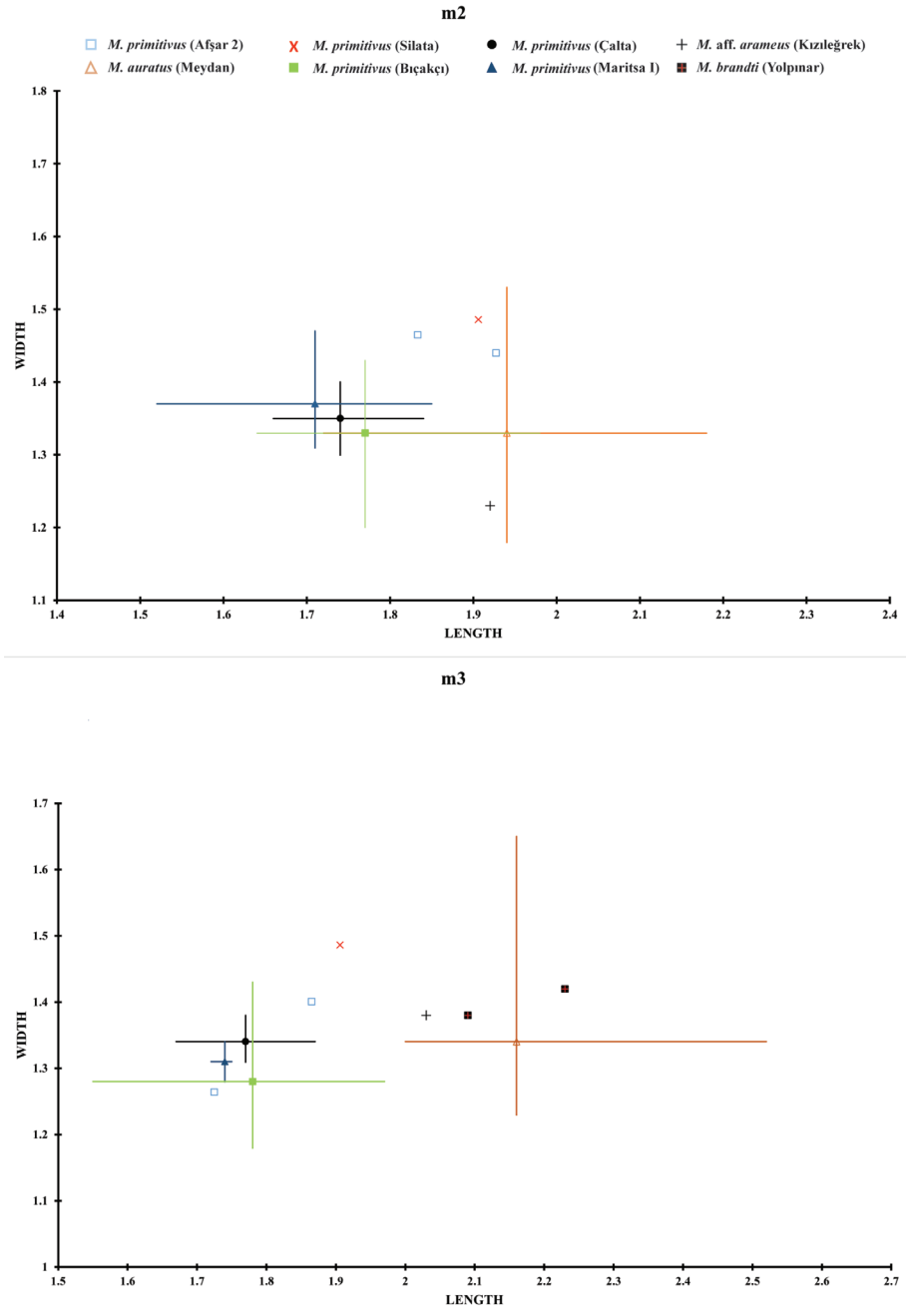

Figure 16. L/W scatter plot of the m2 and m3 from *Mesocricetus primitivus* from Afşar 2, Silata (MN 13/14), Çalta (MN 15), Bıçakçı (MN 17), Maritsa I (MN 15) (De Bruijn et al., 1970; Şen, 1977; Vasileiadou et al., 2003; Hoek Ostende et al., 2015); *M. auratus* from Meydan (Holocene) (Hír, 1992); *M. brandti* from Yolpınar (Early Toringian) and *M.* aff. *arameus* from Kızıleğrek (Early Biharian) (Erturaç et al., 2019). Measurements were made in mm.

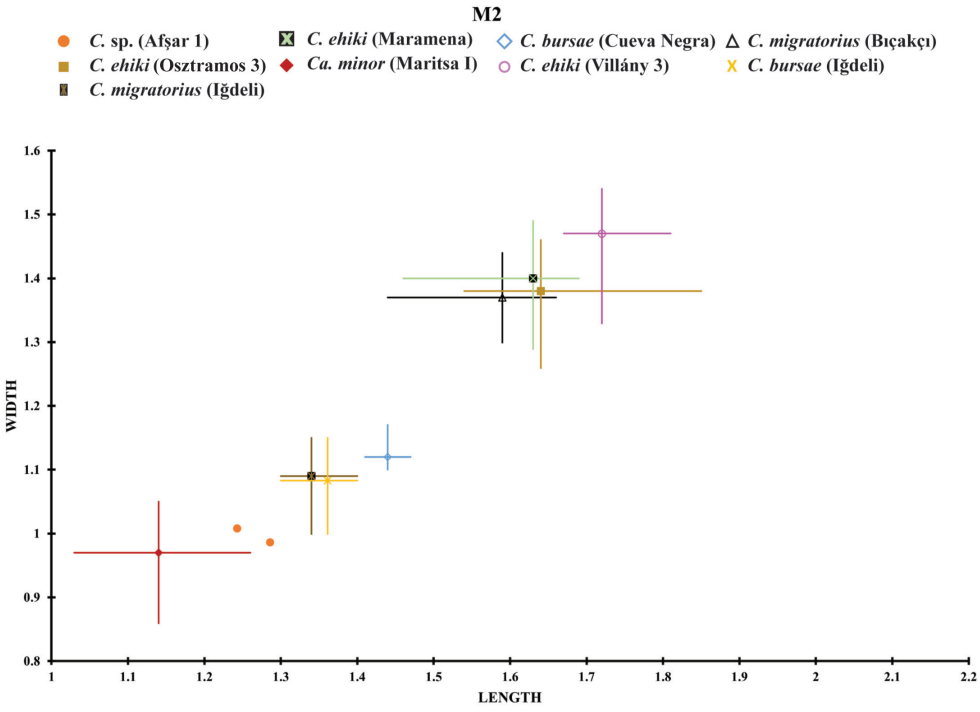

Figure 17. L/W scatter plot of the M2 from *Cricetulus* sp. from Afşar 1; *C. ehiki* from Osztramos 3 (MN 17), Villány 3 (MN 17), Maramena (MN 13) (Daxner-Höck, 1992; Hír, 1993a); *C. migratorius* from Iğdeli (MN 14) and Bıçakçı (MN 17) (Suata-Alpaslan et al., 2010; Hoek Ostende et al., 2015); *C. bursae* from Cueva Negra (late Early Pleistocene) (late Early Pleistocene) and Iğdeli (MN 14) (Suata-Alpaslan et al., 2010; López Jiménez et al., 2018); *Calomyscus* minor, from Maritsa I (MN 13) (De Bruijn et al., 1970). Measurements were made in mm.

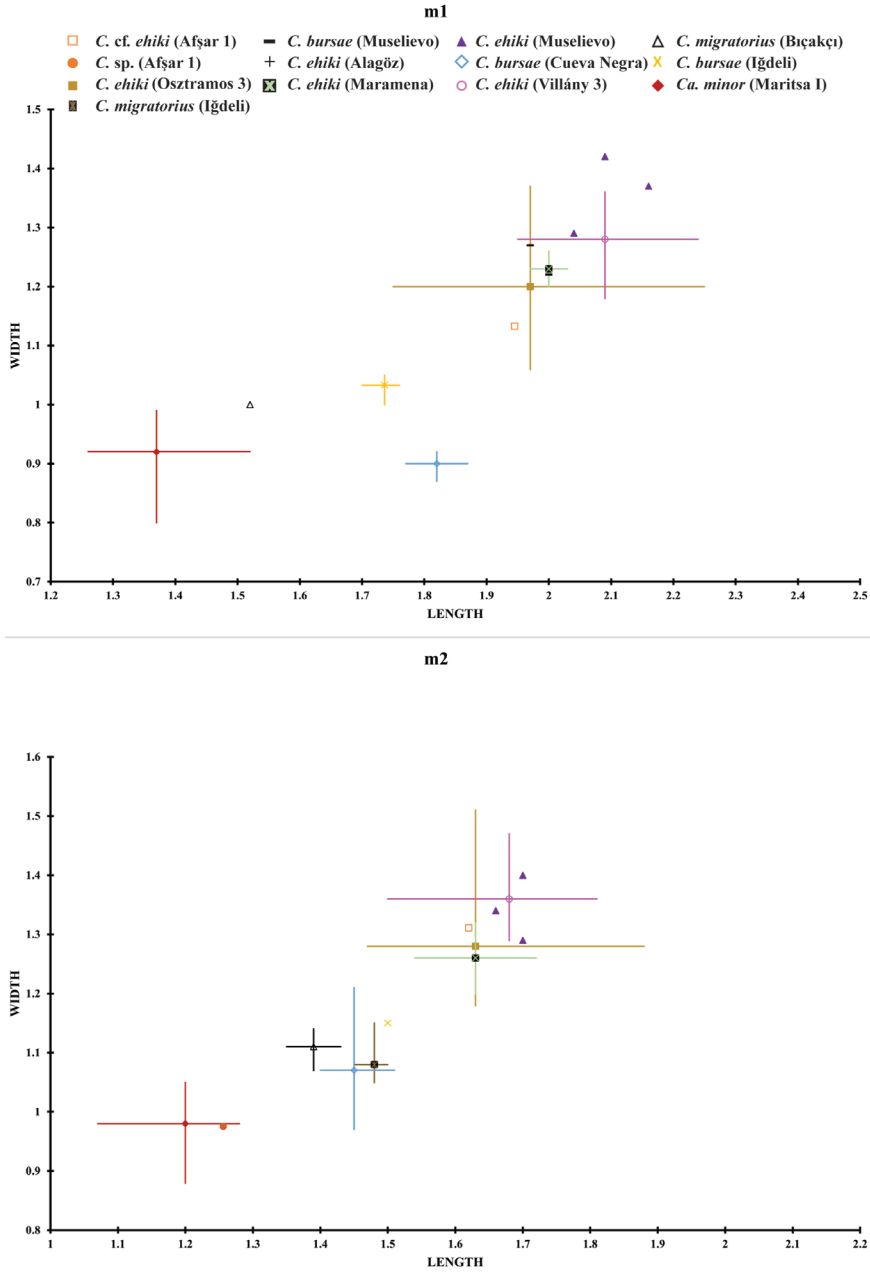

Figure 18. L/W scatter plot of the m1 and m2 from *Cricetulus* cf. *ehiki* and *Cricetulus* sp. from Afşar 1; *C. ehiki* from Osztramos 3 (MN 17), Villány 3 (MN 17), Alagöz (MN 14), Maramena (MN 13), Muselievo (MN 15) (Daxner-Höck, 1992; Hír, 1993a; Popov, 2004; Čermák et al., 2019),; *C. migratorius* from Iğdeli (MN 14) and Bıçakçı (MN 17) (Suata-Alpaslan et al., 2010; Hoek Ostende et al., 2015); *C. bursae* from Cueva Negra (late Early Pleistocene, Iğdeli and Muselievo (Popov, 2004; Suata-Alpaslan et al., 2010; Hoek Ostende et al., 2015); *Calomyscus* minor, from Maritsa I (MN 13) (De Bruijn et al., 1970). Measurements were made in mm.

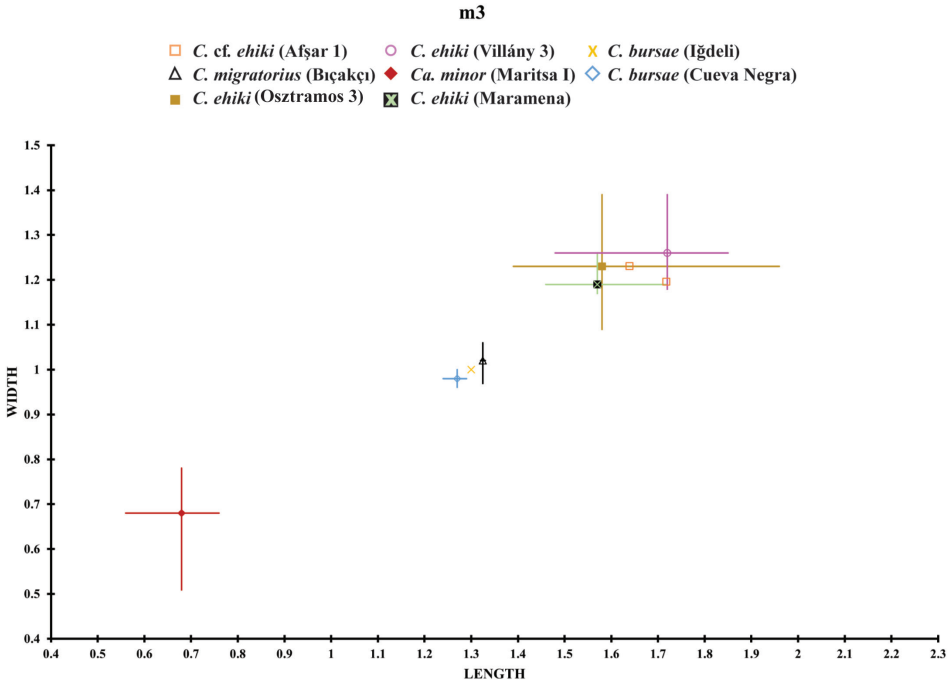

Figure 19. L/W scatter plot of the m3 from *Cricetulus* cf. *ehiki* from Afşar 1; *C. ehiki* from Maramena (MN 13), Villány 3 (Villanyian) (Daxner-Höck, 1992; Hír, 1993a); *C. migratorius* from Bıçakçı (MN 17) (Hoek Ostende et al., 2015); *C. bursae* from Cueva Negra (late Early Pleistocene) and Iğdeli (MN 14) (López Jiménez et al., 2018; Suata-Alpaslan et al., 2010); *Calomyscus minor*, from Maritsa I (MN 13) (De Bruijn et al., 1970). Measurements were made in mm.

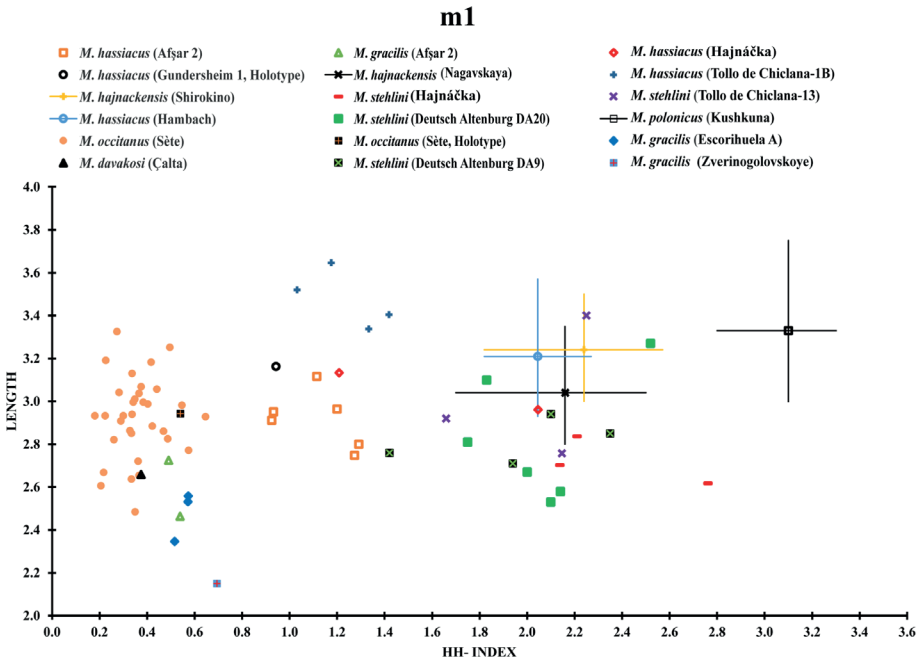

Figure 20. HH-index/L scatter plot of the m1 from *M. hassiacus* from Afşar 2, Gundersheim 1 (MN 16) (Heller, 1936), Hambach (Early Villanyian) (Mörs et al., 1998: figure 19, table 1), Hajnáčka (MN 16) (Fejfar, 1961, original assignment – *M. hajnackensis*) and Tollo de Chiclana-1B (MN 15) (taken from illustration, Minwer-Barakat et al, 2008: figure 2); *M. hajnackensis* from Shirokino (MN 16) and Nagavskaya (MN 16) (Tesakov, 2004: tables 4.2, 4.3, assignment of the present authors – *M. stehlini*); *M. stehlini* from Hajnáčka (Fejfar, 1961), Tollo de Chiclana-13 (MN 16) (taken from illustration, Minwer-Barakat et al., 2008: figure 3), Deutsch Altenburg DA20 (MN 16) and Deutsch Altenburg DA9 (Pliocene) (Rabeder, 1981, original assignment – *M. kretzoii*); *M. occitanus* from Sète (MN 15) (Thaler, 1955; Holotype) and *M. occitanus* from Sète (additional material); *M. gracilis* from Afşar 2, Escorihuela A (MN 15) and Zverinogolovskoye (MN 15/16) (Mein et al., 1990; Pogodina and Strukova, 2016); *M. davakosi* from Çalta (MN 15) (Şen, 1977); *M. polonicus* from Kushkuna (MN 16) (Tesakov, 2004). Measurements were made in mm.

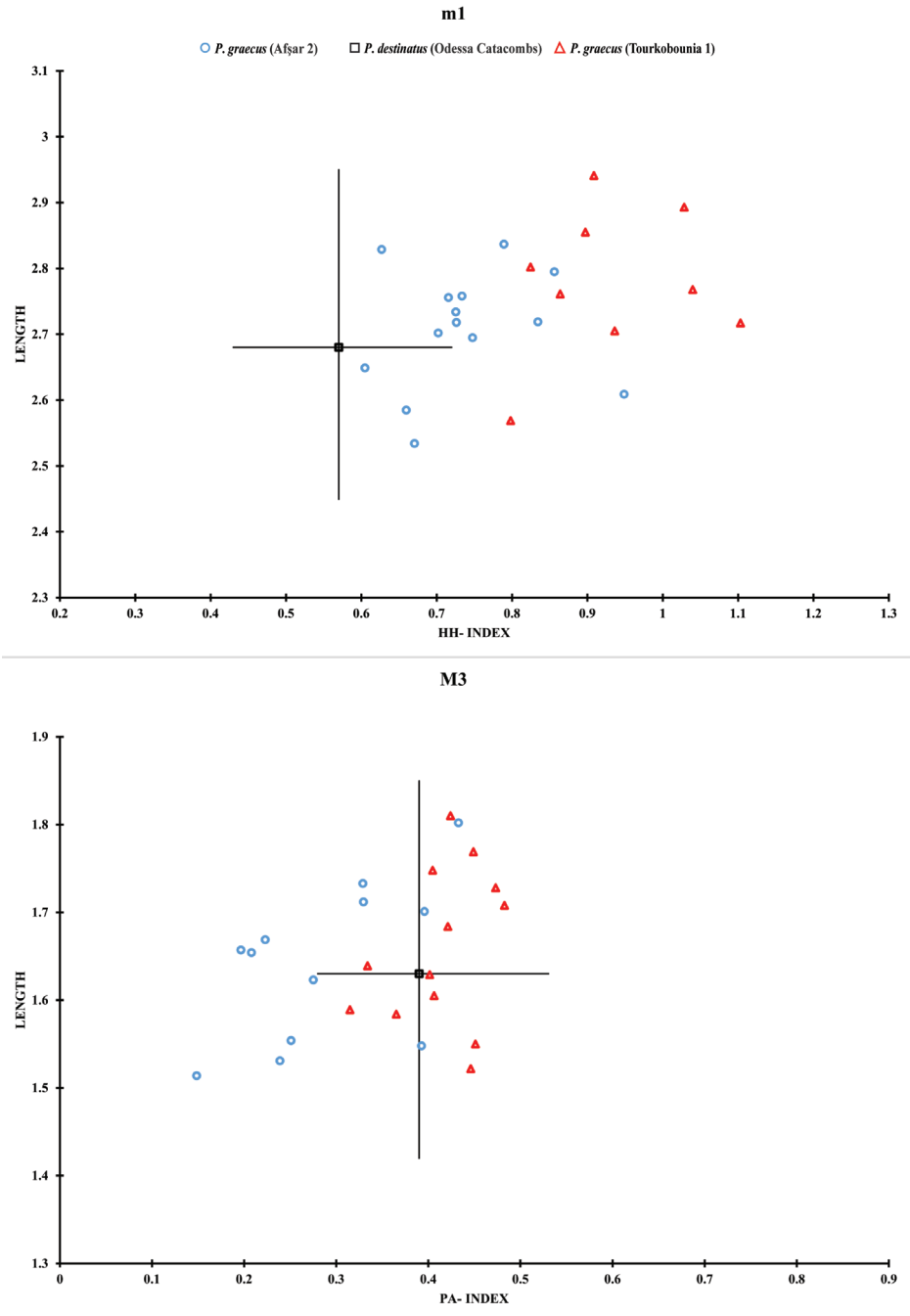

Figure 21. HH-index/L scatter plot of the m1 and PA-index/L of the M3 of *Pliomys graecus* from Afşar 2, Tourkobounia-1 (MN 16) (De Bruijn and Van der Meulen, 1975) and *P. destinatus* from Odessa Catacombs (MN 15) (Tesakov, 2005). Measurements were made in mm.

4. Discussion

Cricetinae and the Arvicolinae species represent a sizable part of the fauna in Afşar. Particularly the latter are considered valuable stratigraphic markers for the Pliocene and Pleistocene. This usage is, however, somewhat hampered by the limited number of comparative metric data of Pliocene vole species in the literature. The morphology and height of the linea sinuosa is an important indicator of the degree of hypsodonty, and a main diagnostic character in Pliocene voles. However, the complete description of this important feature is, particularly in older literature, mostly absent. The issues that arise from these limitations are reflected in the history of the *Mimomys* and *Pliomys* species represented in the Afşar assemblages.

The species *Mimomys hassiacus*, *M. hajnackensis*, *M. occitanus*, and *M. stehlini* have been considered separate species by some authors but synonymized by others (e.g., Ruiz Bustos and Sesé, 1985; Ruiz Bustos, 1987; Fejfar and Storch, 1990). In order to distinguish between these species, we have plotted the m1 length vs the HH-index as an indicator of the height of the enamel-free areas (Figure 20). Mainly based on the HH-index, we distinguish four main groups. The first one includes the species with the lowest enamel-free areas, *M. gracilis* and *M. occitanus*. The second group includes the species *M. hajnackensis* and *M. hassiacus*, including their holotypes from Hajnáčka and Gundersheim-1, respectively. The third one is the group of *M. stehlini* and the last one, with the highest enamel-free areas, the *M. polonicus* group. Notably, the various groups almost completely overlap in the length of the m1. This may have led Ruiz Bustos and Sesé (1985) and Ruiz Bustos (1987) to synonymize the species, as it is clear that in order to differentiate them, the enamel-free areas need to be part of the identification. Fejfar and Storch (1990) synonymized *M. hassiacus* with *M. hajnackensis*, and their suggestion is confirmed, the two species showing a complete overlap. However, one of the two molars from Hajnáčka is included in the *M. stehlini* group, in line with the suggestion of Tesakov (2004) that the type series of *M. hajnackensis* was not homogeneous. Our own study of the material from the Slovakian locality confirmed that this specimen clearly has higher enamel-free areas than the holotype and it should be moved to *M. stehlini*, a species that is also present in the Hajnáčka fauna (Fejfar, 1961). In addition, *M. hassiacus* from Hambach (Mörs et al., 1998) and *M. hajnackensis* from Nagavksaya and Shirokino (Tesakov, 2004) also belong to the *M. stehlini* group, based on the height of the enamel-free areas in these assemblages. The material from Afşar 2 shows an acute shape of the m1's ASD, a feature that is known from the Hajnáčka assemblage but not found in the type series of *hassiacus*. However, since there is no research indicating the intraspecific variation of this character in larger assemblages, its taxonomic validity cannot be assessed and we follow Fejfar and Storch's (1990) suggestion and place Afşar species to *M. hassiacus*.

Mimomys gracilis is the second Arvicolinae of Afşar 2. Its occlusal surface and even its enamel-free areas are similar to *M. occitanus*. The holotype of the latter and the additional material from the locality of Séte have similar morphology and HH-index values with those from *M. gracilis* from Afşar and the locality of Escorihuela A, in Spain (Figure 20). However, the enamel-free areas of *M. occitanus* tend to be lower than

in *M. gracilis*. The main difference between the two species is their dimensions. *Mimomys occitanus* is noticeably larger than *M. gracilis*. Kretzoi (1959) gave neither a complete morphological description of *M. gracilis* nor information on the variation of the species (Şen, 1977). However, the length of *M. gracilis* from the localities of Csarnóta 2, Węże 1, and Nimes varies between 2.5 and 2.84 mm (Şen, 1977, table 8). The species from Afşar is located inside the same range but correlates to the higher length values. Based on the larger size, it is more advanced than the material of Escorihuela A. The most abundant Arvicolinae of the locality, *Pliomys graecus*, was first described by De Bruijn and Van der Meulen (1975). The authors, however, even though they comment about the enamel-free areas, did not provide measurements, as was common at the time. For the current research, we have therefore determined the height range of these enamel-free areas (Figure 21). In addition, we include additional material of *P. graecus*, from the type locality, stored at the Department of Earth Sciences of Utrecht University. *Pliomys graecus* is similar to *P. hungaricus* from the type locality of Carnóta, a species that has been described from an array of localities (Kretzoi, 1959; Fejfar and Storch, 1990; Popov, 2004; Hordijk and De Bruijn, 2009; Hoek Ostende et al., 2015). *Pliomys graecus* and *P. hungaricus* are similar in the height of their enamel- free areas as well as the general morphology of the occlusal surface (De Bruijn and Van der Meulen, 1975). The main difference between the two species lies in the morphology and number of roots of the M3. The two-rooted M3 molars of *P. graecus* with their isolated posterior lobe differentiate the two species. We find the same characters in the arvicoline species of Afşar 2. According to De Bruijn and Van der Meulen (1975), *P. hungaricus* and *P. graecus* may belong to the same phylogenetic lineage with the first being more primitive than the last, based on the higher number of roots on the M3. Remnants of the *Mimomys*-ridge are better developed in more primitive species, like *P. destinatus* and *P. hungaricus*. Based on this, the weak *Mimomys*-ridge found in *P. graecus* of Afşar and the slightly lower enamel-free areas than those from the Greek type locality, indicate a primitive representative of the species.

The present-day Eurasian Cricetinae inhabit mainly steppe environments (Musser Carleton, 1993). The recent species of *Cricetulus* live in an open and dry environment (Blain et al., 2012) and we may presume that its fossil species had the same preference (García-Alix et al., 2008). According to Popov (2004), *Mesocricetus* is indicative of a dry steppe environment. Furthermore, Arvicolinae inhabit the temperate and arctic zones of the Northern hemisphere (Chaline et al., 1999). The presence of these animal groups in Afşar 1 and 2 indicates an open dry environment near the area of deposition, in line with the steppe environment that Jiménez-Moreno et al. (2015) proposed for SW Turkey during the Late Pliocene. A more detailed paleoenvironmental reconstruction can only be made once the entire fauna has been studied.

Afşar 2 is the richer one of the two localities. The large number of its fossil elements led to the identification of *Mimomys gracilis*, *M. hassiacus*, *Pliomys graecus*, and *Mesocricetus primitivus*. The first occurrence of *Mimomys gracilis* is in the MN 15 locality of Wölfersheim (Fejfar and Repenning, 1998; Dahlmann, 2001). It is also part of the MN 15– MN 16 locality of Zverinogolovskoye (Pogodina and Strukova, 2016) and the MN 15 locality of Escorihuela A (Mein et al., 1990, Minwer-Barakat et al., 2008).

Pliomys graecus is part of the MN 16 faunas of Tourkobounia-1 (De Bruijn and Van der Meulen, 1975) and Limni-6 (Koufos, 2006; Vasileiadou and Sylvestrou, 2022) in Greece. However, based on the stage of evolution, the Afşar 2 assemblage seems to be older than the type locality Tourkobounia-1. *Mimomys hassiacus* is present in Europe from MN 15 (upper Ruscinian) to MN 16 (lower Villanyian) (Fejfar et al., 1998; Tesakov, 2004; Sabol et al., 2006). Its first occurrence is in the localities of Węże (Michaux, 1971) and Ivanovce (Fejfar, 1961). *Mesocricetus primitivus* is known from different localities, ranging from the Greek MN 13 locality of Maritsa I (De Bruijn et al., 1970) to the MN 16 locality of Kadiözü in Turkey (Ünay and De Bruijn, 1998). Summarising the different stratigraphic ranges of the species, we preliminarily correlate the locality of Afşar 2 to early MN 16, pending the study of the other faunal elements. Notably, the locality of Hüdaihamami, which is stratigraphically below Afşar 2, has been assigned to MN 17 (Cihan et al., 2003) based on the presence of *Mimomys pliocaenicus*. However, Cihan et al. (2003) only mention the species, without describing it. As we noticed above, the identification of arvicoline fossils requires careful study, including the description and measuring of enamel-free areas. This implies that some older identifications will need to be reviewed in order to improve both datings and our understanding of the faunal development in Anatolia.

Afşar 1 assemblage comprises less material. It is stratigraphically below the MN 16 locality of Gülyazi (Sickenberg et al., 1975) and Afşar 2, which indicates that it is older than these assemblages (Figure 1C). The number and the condition of the fossils from this research do not provide us enough information to confidently correlate Afşar 1 at this point, but the presence of *M.* cf. *gracilis* in combination with its stratigraphic position would place it in MN 15 or early MN 16. The rest of the fauna will be described in a consecutive paper, as part of the PhD project of the first author, and it will provide a better insight into the age of Afşar 1.

5. Conclusion

This paper includes the description of the Arvicolinae and Cricetinae material from the Afşar section in Western Turkey. From the top of the section, in the locality Afşar 2, we distinguished the species *Mimomys hassiacus*, *M. gracilis*, *Pliomys graecus*, *Cricetulus* sp., and *Mesocricetus primitivus*. From Afşar 1, near the base of the section, we recovered *Mimomys* cf. *gracilis*, *Pliomys* sp., Arvicolinae gen. et sp. indet. and *Cricetulus* cf. *ehiki*. This material indicates the presence of dry and open spaced habitats and places the locality of Afşar 2 to early MN 16 with Afşar 1 indicating similar or even older age so far, pending the study of the other faunal elements.

Acknowledgments

We express our gratitude to the Museum of Natural History of Ege University in İzmir and especially Prof. Dr. Tanju Kaya and her staff for their hospitality. Furthermore, we would also like to thank Peter Joniak from the Department of Geology and Paleontology of the Comenius University in Bratislava, for his assistance in the field as well as giving us access to literature and material from the Slovak National Museum and helping us reach the eastern part of the country in order to visit the collection of Rimavská Sobota. In addition, we would like to thank him for his warm welcome of PS in Slovakia. We thank Martin Sabol from the same institution, for providing us with material from the Slovak National Museum and his support during the visit of PS to Bratislava. We are grateful for the help of Yanell Braumuller, Melike Bilgin, Rutger van den Hoek Ostende and Mark Doeland for their essential assistance in collecting and processing the material in the field. We express our gratitude to Wilma Wessels from the Department of Geology of Utrecht University, for her constant help by giving us access to the rich collections of her Department. We would like to thank Pablo Peláez- Campomanes from the Museo Nacional de Ciencias Naturales in Madrid, Spain, for his guidance in the field and for providing us with rare publications. We also thank Eelco Kruidenier from Naturalis Biodiversity Center, for helping us collect part of our specimens. We would like to thank the Head of Section Paleomammalogy in Senckenberg Research Institute, Thomas Lehmann, for the detailed pictures from the holotype of *Mimomys hassiacus*. Furthermore, we express our gratitude to Mehdi Mouana from Institut des Sciences de l'Evolution de Montpellier, for providing us with pictures from the holotype of *M. occitanus*. We would like to thank Doris Nagel for giving us access to the collection from the Institut für Paläontologie of the University of Vienna, in Austria and her hospitality during the visit of the first author in Vienna. Last but not least, we would like to thank Professor Şevket Şen and the two anonymous reviewers for their suggestions that significantly improved the manuscript.

References

Alçiçek MC, Mayda S, Veen JH ten, Boulton SJ, Neubauer TA et al. (2019). Reconciling the stratigraphy and depositional history of the Lycian orogen-top basins, SW Anatolia. Palaeobiodiversity and Palaeoenvironments 99: 551-570. https://doi.org/10.1007/ s12549-019-00379-2

Suata-Alpaslan F, Ünay E, Ay F (2010). Igdeli (Gemerek, Sivas) lokalitesi Erken Pliyosen fauna istifinin Rodentia ve Lagomorpha (Mammalia) fosilleri: biyokronolojik ve paleobiyocografik anlamlari: C.Ü. Fen-Edebiyat Fakultesi, Fen Bilimleri Dergisi 31: 1-29 (in Turkish).

Argyropulo AI (1932). Preliminary Description of Two New Palearctic Voles. Journal of Mammalogy 13 (3): 268-271.

Bachelet B. Esteban-Aenlle J, López-Martínez N (1991). Révision des populations de *Mimomys* de petite taille (Rodentia, Mammalia) du Pliocène supérieur d'Europe sud-occidentale. Geobios 22 (3): 349-360 (in French). https://doi.org/10.1016/ S0016-6995(09)90014-6

Balcı V (2011). 1/100 000 ölçekli Türkiye Jeoloji Haritaları, Afyon-L25 paftası: Maden Tetkik ve Arama Genel Müdürlüğü. Jeoloji Etüdleri Dairesi Yayını No: 161, Ankara, Türkiye (in Turkish).

Bilgin M, Joniak P, Mayda S, Göktaş F, Pelaez Campomanes P, Hoek Ostende, LW van den (2021). Micromammals from the late early Miocene of Çapak (western Anatolia) herald a time of change. Journal of Paleontology 95 (5): 1079-096. https://doi. org/10.1017/jpa.2021.27

Bilgin M, Joniak P, Pelaez Campomanes P, Göktaş F, Mayda S, Lorinser C, Wijbrans J, Kaya T, Hoek Ostende, LW van den (2022). Beydere 3: a new early Miocene small mammal assemblage from the western Anatolia, Turkey. Historical Biology 1-20. https://doi.org/10.1080/08912963.2022.2077646

Blain HA, Sesé C, Rubio-Jara S, Panera J, Uribelarrea D, Pérez- González A (2012). Paleoenvironmental and paleoclimatic reconstruction of the early Late Pleistocene (MIS 5a) in central Spain: the small vertebrates (Amphibia, Reptilia & Mammalia) from the sites of Hat and Preresa. Quaternaire 24 (2): 191-205 (in French). https://doi.org/10.4000/quaternaire.6604

Bowdich TE (1821). An Analysis of the Natural Classifications of Mammalia for the Use of Students and Travellers, Smith J. Paris, France. pp. 115.

Čermák S, Joniak P, Rojay B (2019). A new early Pliocene locality Tepe Alagöz (Turkey) reveals a distinctive tooth phenotype of *Trischizolagus* (Lagomorpha, Leporidae) in Asia Minor. Palaeontologia Electronica 22.1.14A: 1-21. https://doi. org/10.26879/924

Čermák S, Wagner J, Fejfar O, Horáček I (2007). New Pliocene localities with micromammals from the Czech Republic: a preliminary report. Fossil Record 10 (1): 60-68. https://doi. org/10.1002/mmng.200600019

Chaline J, Brunet-Lecomte P, Montuire S, Viriot L, Courant F (1999). Anatomy of the arvicoline radiation (Rodentia): palaeogeographical, palaecoecological history and evolutionary data. Annales Zoologici Fennici 36: 239-267.

Cihan M, Saraç G, Gökçe AO (2003). Insights into biaxial extensional tectonics: an example from the Sandıklı Graben, West Anatolia, Turkey. Geological Journal 38: 47-66. https://doi.org/10.1002/ gj.928

Cuenca-Bescós G (2003). Análisis filogenético de *Allocricetus* del Pleistoceno (Cricetidae, Rodentia, Mammalia). Coloquios de Paleontologia 1: 95-113 (in Spanish).

Dahlmann T (2001). Die Kleinsäuger der unter-pliozänen Fundstelle Wölfersheim in der Wetterau (Mammalia: Lipotyphla, Chiroptera, Rodentia). CFS Courier Forschungsinstitut Senckenberg 227: 1-129 (in German).

Daxner-Höck G (1992). Die Cricetinae aus dem Obermiozän von Maramena (Mazedonien, Nordgriechenland). Paläontologische Zeitschrift 66 (3/4): 331-367 (in German).

De Bruijn H, Van der Meulen AJ (1975). The early Pleistocene rodents from Tourkobounia-1 (Athens, Greece). Proceedings Koninklijke Nederlandse Akademie van Wetenschappen Series B 78: 314-338.

De Bruijn H, Dawson MR, Mein P (1970). Upper Pliocene Rodentia, Lagomorpha and Insectivora (Mammalia) from the isle of Rhodes (Greece). 3. The Rodentia, Lagomorpha and Insectivora. Proceedings of the Koninklijke Nederlandse Akademie van Wetenschappen Series B 73 (5): 568-584.

De Bruijn H, Mayda S, Hoek Ostende LW van den, Kaya T, Saraç G (2006). Small mammals from the Early Miocene of Sabuncubeli (Manisa, S.W. Anatolia, Turkey). Beiträge zur Paläontologie von Österreich 30: 57-87.

Demirel FA, Mayda S, Alçiçek MC, Eryılmaz D (2019). Burdur ve Afyonkarahisar İlleri ve İlçelerinde Neojen ve Pleistosen Dönem Fosil Lokalitelerinin Tespiti Yüzey Araştırması-2017. Araştırma Sonuçları Toplantısı 36 (1): 193-202 (in Turkish).

Eronen JT, Ataabadi MM, Micheels A, Karme A, Bernor, RL, Fortelius M (2009). Distribution history and climatic controls of the Late Miocene Pikermian chronofauna. Proceedings of the National Academy of Sciences of the United States of America 106: 11867-11871.

Erturaç MK, Erdal O, Sunal G, Tüysüz O, Şen S (2019). Quaternary evolution of the Suluova Basin: implications on tectonics and palaeonvironments of the Central North Anatolian Shear Zone. Canadian Journal of Earth Sciences 56: 1239-1262. https://doi. org/10.1139/cjes-2018-0306

Fejfar O (1961). Die Plio-Pleistozänen Wirbeltierfaunen von Hajnáčka und Ivanovce (Slowakei), CSR. 2. Microtidae und Cricetidae inc. sed., Neues Jahrbuch für Geologie und Paläontologie 112 (1): 48-82 (in German).

Fejfar O, Storch G (1990). Eine Pliozäne (ober-Ruscinische) Kleinsäugerfauna aus Gundersheim, Rheinhessen-1. Nagetiere: Mammalia, Rodentia. Senckenbergiana Lethaea 71: 139-184 (in German).

Fejfar O, Repenning CA (1998). The ancestors of the lemmings (Lemmini, Arvicolinae, Cricetidae, Rodentia) in the early Pliocene of Wölfersheim near Frankfurt am Main; Germany. Senckenbergiana lethaea 77 (1-2): 161-193. https:// doi. org/10.1007/BF03043739

Fejfar O, Heinrich WD, Lindsay EH (1998). Updating the Neogene rodent biochronology in Europe. Mededelingen Nederlands Instituut voor Toegepaste Geowetenschappen TNO 60: 533- 554.

Fischer G (1817). Adversaria zoologica. Mémoires de la Société Impériale des Naturalistes de Moscou 5: 357-472 (in French).

Forsyth Major FCI (1902). Exhibition of, and remarks upon some jaws and teeth of Pliocene voles (*Mimomys* gen. nov.). Proceedings Zoological Society 1: 102-107.

García-Alix A, Minwer-Barakat R, Martín Suárez E, Freudenthal M, Martín JM (2008). Late Miocene–Early Pliocene climatic evolution of the Granada Basin (southern Spain) deduced from the paleoecology of the micromammal associations. Palaeogeography Palaeoclimatology Palaeoecology 265(3-4): 214-225. https://doi.org/10.1016/j. palaeo.2008.04.005

Gray JE (1821). On the natural arrangement of vertebrose animals. London Medical Repository 15: 296-310.

Heller F (1936). Eine oberpliocäne Wirbeltierfauna aus Rheinhessen. Neues Jahrbuch für Mineralogie, Geologie und Paläontologie, Abteilung B, Beilageband 76: 99-160 (in German).

Hír J (1989). Revised investigation of the *Allocricetus* material of Tarkő Rock Shelter. Folia Historico-Naturalia Musei Matraensis 14: 43-72.

Hír J (1992). Subfossil *Mesocricetus* population from the Toros Mountains (Turkey) (Mammalia). Folia Historico Naturalia Musei Matraensis 17: 107-130.

Hír J (1993a). *Allocricetus ehiki*, SCHAUB, 1930 (Rodentia, Mammalia) finds from Villány 3 and Osztramos 3 (Hungary). Fragmenta Mineralogica et Paleontologica 16: 61-80.

Hír J (1993b). *Cricetulus migratorius* (PALLAS 1773) (Rodentia, Mammalia) population from the Toros Mountains (Turkey) (with a special reference to the relation of *Cricetulus* and *Allocricetus* genera). Folia Historico Naturalia Musei Matraensis 18: 17-34.

Hoek Ostende LW van den, Casanovas-Vilar I, Furió M (2020). Stuck in the middle. A geographical appraisal of the oldest insectivores and a marsupial from the Vallès-Penedès Basin (early Miocene, Catalonia, Spain). Comptes Rendus Palevol 19 (1): 1-25.

Hoek Ostende LW van den, Diepenveen F, Tesakov A, Saraç G, Mayhew D et al. (2015). On the brink: micromammals from the latest Villanyian from Bıçakçı (Anatolia). Geological Journal 50: 230-245. https://doi.org/10.1002/gj.2622

Hordijk K, De Bruijn H (2009). The succession of rodent faunas from the Mio/Pliocene lacustrine deposits of the Florina-Ptolemais- Servia Basin (Greece). Hellenic Journal of Geosciences 44: 21- 103.

Illiger C (1811). Prodromus systematis mammalium et avium additis terminis zoographicis utriusque classis, eorumque versione germanica. Salfeld C. Berlin, Germany: pp. 301 (in Latin)

Jiménez-Moreno G, Suc JP, Fauquette S (2010). Miocene to Pliocene vegetation reconstruction and climate estimates in the Iberian Peninsula from pollen data. Review of Palaeobotany and Palynology 162: 403-415. https://doi.org/10.1016/j. revpalbo.2009.08.001

Jiménez-Moreno G, Rodríguez-Tovar FJ, Pardo-Igúzquiza E, Fauquette S, Suc JP et al. (2005). High-resolution palynological analysis in late early–middle Miocene core from the Pannonian Basin, Hungary: climatic changes, astronomical forcing and eustatic fluctuations in the Central Paratethys. Palaeogeography Palaeoclimatology Palaeoecology 216: 73-97. https://doi.org/10.1016/j.palaeo.2004.10.007

Jiménez-Moreno G, Alçiçek H, Alçiçek MC, Hoek Ostende LW van den, Wesselingh FP (2015). Vegetation and climate changes during the late Pliocene and early Pleistocene in SW Anatolia, Turkey. Quaternary Research 84: 448-456. https://doi. org/10.1016/j.yqres.2015.09.005

Kaya O, Ünay E, Göktaş F, Saraç G (2007). Early Miocene stratigraphy of central west Anatolia, Turkey: implications for the tectonic evolution of the eastern Aegean area. Geological Journal 42: 85-109. https://doi.org/10.1002/gj.1071

Kormos T (1931). Oberpliozän Wühlmäuse von Senèze (Haute-Loire) und Val d'Arno (Toscana). Abhandlungen der Schweizerische Paläontologische Gesellschaft 51: 11-14 (in German).

Kormos T (1934). Neue Insektenfresser, Fledermäuse und Nager aus dem Oberpliozän der Vilányer Gegend. Földtani Közlony 64: 296-321 (in German).

Koufos GD (2006). The Neogene mammal localities of Greece: faunas, chronology and biostratigraphy. Hellenic Journal of Geosciences 41:183-214.

Koufos GD (2013). Neogene mammal biostratigraphy and chronology of Greece. In: Wang X, Flynn LJ, Fortelius M (editors). Fossil mammals of Asia. Neogene biostratigraphy and chronology. New York: Columbia University Press, pp. 595-621. https://doi. org/10.7312/columbia/9780231150125.003.0028

Koufos GD (2016). Neogene and Quaternary continental biostratigraphy of Greece based on mammals. Bulletin of the Geological Society of Greece 50 (1): 55-64.

Koufos GD, Vasileiadou K (2015). Miocene/Pliocene mammal faunas of southern Balkans: implications for biostratigraphy and palaeoecology. Palaeobiodiversity and Palaeoenvironments 95: 285-303. https://doi.org/10.1007/s12549-015-0201-4

Kowalski K (1960). Pliocene Insectivores and Rodents from Rebielice Królewskie (Poland). Acta Zoologica Cracoviensia 5: 155-200.

Kowalski K (2001). Pleistocene rodents of Europe. Folia Quaternaria 72: 1-389.

Kretzoi M (1956). Die alt pleistozänen Wirbeltierfaunen des Villanyer gebirges. Geologica Hungarica Series Palaeontologica 27: 1-264 (in German).

Kretzoi M (1959). Insectivoren, Nagetiere und Lagomorphen der jüngstpliozänen Fauna von Csarnóta im Villáyer Gebirge (Südungarn). Vertebrata Hungarica 1 (2): 237-246 (in German).

Leske NG (1779). Anfangsgründe der Naturgeschichte. Leipzig: S.L. Crusius (in German).

López-Guerrero P, García-Paredes I, Álvarez-Sierra MA (2013). Revision of *Cricetodon soriae* (Rodentia, Mammalia), new data from the middle Aragonian (middle Miocene) of the Calatayud-Daroca basin (Zaragoza, Spain). Journal of Vertebrate Paleontology 33: 169-184. https://doi.org/10. 1080/02724 634. 2012. 716112.

López Jiménez A, Haber Uriarte M, López Martínez M, Walker MJ (2018). Small-mammal indicators of biochronology at Cueva Negra del Estrecho del Río Quípar. Historical Biology 32 (2):18-33. https://doi.org/10.1080/08912963.2018.1462804

Maul L, Masini F, Abbazzi L, Turner A (1998). The use of different morphometric data for absolute age calibration of some South and Middle European arvicolid populations. Palaeontographia Italica 85: 111-151.

Mayhew DF (1978). Late Pleistocene small mammals from Arnissa (Macedonia, Greece). Proceedings of the Koninklijke Nederlandse Akademie van Wetenschappen B 81: 302-321.

Mayhew DF, Dieleman FE, Boele J, Verhaard L, Hoek Ostende LW van den (2008). *Mimomys hajnackensis* from the Pliocene of the Netherlands. Netherlands Journal of Geosciences. Geologie en Mijnbouw 87 (2): 181-188. https://doi.org/10.1017/ S0016774600023210

Méhely von L (1914). Fibrinae Hungariae. Annales Historico- Naturales Musei Nationalis Hungarici 12: 157-243. (in Hungarian and in German)

Mein P, Moissenet E, Adrover R (1990). Biostratigraphie du Néogène Supérieur du bassin de Teruel. Paleontologia i Evolució 23: 121-139. (in French)

Michaux J (1971). Arvicolidae (Rodentia) du Pliocène terminal et du Quaternaire ancien de France et d'Espagne. Palaeovertebrata 4: 137-214 (in French). https://doi.org/10.18563/pv.4.5.137-214

Miller GS (1910). Two new genera of murine rodents. Smithsonian Miscellaneous Collection 52: 497-498.

Milne-Edwards A (1867). Description de quelques espèces nouvelles d' Écureuils de l'ancien continent. Revue et Magasin de Zoologie pure et appliquée 2 (19): 225-234 (in French).

Minwer-Barakat R, García-Alix A, Martín Suárez E, Freudenthal M (2004). Arvicolidae (Rodentia) from the Pliocene of Tollo de Chiclana (Granada, SE Spain). Geobios 37: 619-629. https:// doi.org/10.1016/j.geobios.2004.05.001

Minwer-Barakat R, García-Alix A, Martín-Suárez E, Freudenthal M (2008). The Latest Ruscinian and Early Villanyian Arvicolinae from Southern Spain Re-Examined: Biostratigraphical Implications. Journal of Vertebrate Paleontology 28 (3): 841-850. https://doi.org/10.1671/0272-4634(2008)28[841:TLRAE V]2.0.CO;2

Mörs T, Koenigswald W Von, Hocht F Von der (1998). Rodents (Mammalia) from the late Pliocene Reuver Clay of Hambach (Lower Rhine Embayment, Germany). In: Van Kolfschoten T, Gibbard PL (editors). The Dawn of the Quaternary. Mededelingen Nederlands Instituut voor Toegepaste Geowetenschappen TNO 60: 135-160.

Musser GG, Carleton MD (1993). Family Muridae. In: Wilson DE, Reeder DM (editors). Mammal Species of the World. A Taxonomic and Geographic Reference. 2nd ed. Washington, USA: Smithsonian Institution Press and The American Society of Mammalogists, pp. 501-755.

Nehring A (1898). Über *Cricetus*, *Cricetulus* und *Mesocricetus* n. Subg. Zoologischer Anzeiger 21: 493-495 (in German).

Nesin VA (1983). New finds of fossil voles of the genus *Pliomys* (Rodentia, Microtidae). Vestnik Zoologii 6: 41-45 (in Russian).

Ognev SI (1914). Mammals of lower reaches of the river Tuman Gana (southern Primorye district). Part 1. Rodents (Rodentia). Dnevnik Zoologičeskogo Otdelenia Obšestva Lûbitelej Estestvoznaniâ, Antropologii i Etnografii 2 (3): 101-128 (in Russian).

Pogodina NV, Strukova TV (2016). Primitive Arvicolids (Early – Middle Pliocene) from Zverinogolovskoye locality (Southern Trans-Urals region). Quaternary International 420: 171-177. https://doi.org/10.1016/j.quaint.2015.10.083

Popescu SM, Biltekin D, Winter H, Suc JP, Melinte-Dobrinescu MC et al. (2010). Pliocene and Lower Pleistocene vegetation and climate changes at the European scale: long pollen records and climatostratigraphy. Quaternary International 219 (1-2): 152-167. https://doi.org/10.1016/j.quaint.2010.03.013ostebruijn

Popov V (2004). Pliocene small mammals (Mammalia, Lipotyphla, Chiroptera, Lagomorpha. Rodentia) from Muselievo (North Bulgaria). Geodiversitas 26: 403-491.

Rabeder G (1981). Die Arvicoliden (Rodentia, Mammalia) aus dem Pliozän und dem älteren Pleistozän von Niederösterreich. Beiträge zur Paläontologie von Österreich 8: 1-373 (in German).

Rabeder G (1988). Die Arvicoliden (Rodentia, Mammalia) aus dem Ältest-Pleistozän von Schernfeld (Bayern). Beiträge zur Paläontologie von Österreich 14: 123-237 (in German).

Ruiz Bustos A (1987). Consideraciones sobre la sistemática y evolución de la Familia Arvicolidae. El género Mimomys. Paleomammalia 1: 1-54 (in Spanish).

Ruiz Bustos A, Sesé C (1985). Evolución de los géneros *Mimomys*, *Arvicola* y *Allophaiomys* (Arvicolidae, Rodentia, Mammalia) en el Plioceno y Pleistoceno de la Península Ibérica. Estudios Geológicos 41: 99-104 (in Spanish).

Sabol M, Konečný V, Vass D, Kováčová M, Ďurišová A et al. (2006). Early Late Pliocene site of Hajnáčka I (Southern Slovakia)- Geology, palaeovolcanic evolution, fossil assemblages and palaeoenvironment. Courier Forschungsinstitut Senckenberg 256: 261-274.

Saraç G (2003). Vertebrate fossil localities of Turkey. Scientific Report No. 10609. Ankara, Turkey: The General Directorate of the Mineral Research and Exploration of Turkey (MTA).

Schaub S (1930). Quartäre und jungtertiäre Hamster. Abhandlungen der Schweizerischen paläontologischen Gesellschaft 49 (6): 1-49 (in German).

SchevtschenkoAl (1965). Faunistic complexes of small mammals from upper Cenozoic deposits in the south-western part of the Russian plains. In: Nikiforova KV, Peine AV, Kuznetzova KJ, Menner VV, Timofeev PP (editors). Stratigraphie importance of small mammalian Anthropogene fauna. Moscou: Nauka, pp. 7-59 (in Russian).

Şen S (1977). La faune de rongeurs pliocène de Çalta (Ankara, Turquie). Bulletin du Muséum National d'Histoire Naturelle, Sciences de la Terre 61: 89-171 (in French).

Sickenberg O, Becker-Platen JD, Benda L, Berg D, Engesser B et al. (1975). Die Gliederung des höheren Jungtertiärs und Altquartärs in der Türkei nach Vertebraten und ihre Bedeutung für die internationale Neogen-Stratigraphie. Geologisches Jahrbuch Reihe B, Hefte 15: 1–167 (in German).

Suc JP, Popescu SM (2005). Pollen records and climatic cycles in the North Mediterranean region since 2.7 Ma. Geological Society of London, Special Publication 247: 147-158. https://doi. org/10.1144/GSL.SP.2005.247.01.08

Tesakov AS (2004). Biostratigraphy of middle Pliocene-Eopleistocene of eastern Europe (based on small mammals). Transactions of the Geological Institute 554. Moscow, Russia: Russian Academy of Sciences, Nauka (in Russian).

Tesakov AS (2005). Pliocene voles (*Pliomys*, Arvicolinae, Rodentia) from the Odessa Catacombs. Russian Journal of Theriology 4 (2): 123-135. https://doi.org/10.15298/rusjtheriol.4.2.05

Thaler L (1955). Sur l'âge Pliocène de la faune des grottes du Lazaret (Sète, Hérault). Comptes Rendus de l' Académie des Sciences 241: 433-435 (in French).

Thomas O (1917). On the small Hamsters that have been referred to *Cricetulus phaeus* and *campbelli*. Annals and Magazine of Natural History, Series 8, 19: 456-457.

Topachevsky VA, Scorik AF (1967). *Dolomys* (*Pliomys*) *ucrainicus* sp. n. (Rodentia, Microtidae) from the upper Pliocene deposits of the south of the Ukraine. Institute of Zoology, Academy of Sciences, Ukrainian SSR. pp. 1-67.

Turan N (2002. Geological map of Turkey in 1:500000 scale: Ankara sheet. Publication of Mineral Research and Exploration Directorate of Turkey (MTA), Ankara.

Ünay E, De Bruijn H (1998). Plio-Pleistocene rodents and lagomorphs from Anatolia. Mededelingen Nederlands Instituut voor Toegepaste Geowetenschappen TNO 60: 431-466.

Van der Meulen AJ (1973). Middle Pleistocene smaller mammals from the Monte Peglia, (Orvieto, Italy) with special reference to the phylogeny of *Microtus* (Arvicolidae, Rodentia). Quaternaria 17: 1-144.

Vasileiadou K, Sylvestrou I (2022). The Fossil Record of Rodents (Mammalia: Rodentia) in Greece. In: Vlachos E (editors). Fossil Vertebrates of Greece Vol. 1 –basal vertebrates, amphibians, reptiles, afrotherians, glires, and primates. Cham: Springer – Nature Publishing Group. pp. 407-610.

Vasileiadou K, Koufos GD, Syrides GE (2003). Silata, a new locality with micromammals from the Miocene / Pliocene boundary of the Chalkidiki peninsula, Macedonia, Greece. Deinsea, 10 (1): 549–562.

Zdansky O (1928). Die Säugetiere der Quartärfauna von Chou-K'ou- Tien. Palaeontologia Sinica, Series C, 5 (4): 1-146 (in German).

Zhang Y, Jin C, Kawamura Y (2010). A distinct large vole lineage from the Late Pliocene – Early Pleistocene of China. Geobios 43: 479-490. https://doi.org/10.1016/j.geobios.2010.01.005

Supplementary material

Table 1. Material and measurements of *Mimomys occitanus* from the locality of Sète (additional material) stored in the Department of Earth Sciences in Utrecht University, in the Netherlands.*

m1	N	Min	Max	Mean	Std.Dev.	Std.error
Length	33	2.49	3.33	2.92	0.19	0.03
Width	33	1.11	1.64	1.41	0.13	0.02
ASD	18	0.52	1.13	0.82	0.15	0.04
HSD	26	0.21	0.57	0.34	0.09	0.02
HSLD	31	0.11	0.30	0.22	0.05	0.01
AL	32	33.25	49.88	43.27	4.68	0.83
HH- index	34	0.18	0.65	0.36	0.11	0.02

*Measurements were made in mm.

Table 2. Material and measurements of *Mimomys gracilis* from the locality of Escorihuela A (Mein et al., 1990) stored in the Department of Earth Sciences in Utrecht University, in the Netherlands.

m1	N	Min	Max	Mean	Std.Dev.	Std.error
Length	4	2.35	2.75	2.55	0.16	0.08
ASD	4	0.79	1.14	0.91	0.16	0.08
HSD	5	0.41	0.53	0.47	0.05	0.02
HSLD	4	0.21	0.28	0.25	0.03	0.02
AL	4	36.85	44.46	39.20	3.53	1.77
HH- index	4	0.52	0.57	0.55	0.03	0.01

*Measurements were made in mm.

Table 3. Material and measurements of *Pliomys graecus* from the locality of Tourkobounia 1 (De Bruijn and Van der Meulen, 1975) stored in the Department of Earth Sciences in Utrecht University, in The Netherlands.

m1	N	Min	Max	Mean	Std.Dev.	Std.error
Length	14	2.57	3.07	2.82	0.16	0.04
ASD	10	0.77	1.47	1.07	0.19	0.06
HSD	10	0.66	0.97	0.77	0.10	0.03
HSLD	13	0.34	0.70	0.48	0.11	0.03
HH- index	10	0.80	1.10	0.93	0.10	0.03
M3	**N**	**Min**	**Max**	**Mean**	**Std.Dev.**	**Std.error**
Length	19	1.50	1.81	1.65	0.08	0.02
AS	16	0.14	0.35	0.20	0.05	0.01
PRS	16	0.23	0.44	0.35	0.06	0.01
PA- index	14	0.31	0.48	0.41	0.05	0.01

*Measurements were made in mm.